Environmental and Experimental Botany 209 (2023) 105313

Contents lists available at ScienceDirect

Environmental and Experimental Botany

journal homepage: www.elsevier.com/locate/envexpbot

How does particulate matter affect plant transcriptome and microbiome?

Chiara Vergata [a,1], Felice Contaldi [a,1], Ivan Baccelli [b], Marcos Fernando Basso [a,b], Alberto Santini [b], Francesco Pecori [b], Matteo Buti [c], Alessio Mengoni [a], Francesca Vaccaro [a], Barbara Basso Moura [d], Francesco Ferrini [c], Federico Martinelli [a,b,*]

[a] Department of Biology, University of Florence, 50019 Sesto Fiorentino, Italy
[b] Institute for Sustainable Plant Protection, National Research Council of Italy, Sesto Fiorentino, 50019 Florence, Italy
[c] Department of Agriculture, Food, Environmental and Forestry Sciences, Section Woody Plants, University of Florence, 50019 Sesto Fiorentino, Italy
[d] Institute of Research on Terrestrial Ecosystems (IRET), National Research Council of Italy (CNR), Via Madonna del Piano 10, 50019 Sesto Fiorentino, Italy

ARTICLE INFO

Keywords:
Particulate matter
RNA-seq
Photinia x fraseri
Co-expression analysis

ABSTRACT

Phylloremediation for the reduction of air particulate matter (PM) is an interesting opportunity to significantly contribute to improve the air quality of urban environment. The aim of this study was to: 1) gain insight into the gene regulatory networks modulating leaf responses to polluted air, 2) identify possible changes in the leaf microbiome due to particulate matter in the real urban environment. The leaf transcriptome and microbiome were analyzed for *Photinia* x *fraseri* L. plants cultivated for three months in pots in two close-by areas under different levels of air PMs (low and high). PCA and heat map analysis showed that 28 differentially expressed genes in common between the three pairwise comparisons were able to clearly discriminate plants under higher PM levels. The pollutants were mainly sensed by plants through a restructuring modification of cell wall and membrane due to the main repression of lipid desaturases. In addition, high PMs showed a clear repression of genes belonging to primary metabolism pathways involved in C assimilation. Microbiome analysis showed no significant changes in taxonomic diversity indexes for the bacterial communities, whereas fungi belonging to the genera *Epicoccum* and *Dioszegia* were differently affected by the different exposure to PM levels. A model of transcriptional regulation to air PMs in plants has been proposed.

1. Introduction

The use of plants as phylloremediation is a growing interest field, considering that a high percentage of the global population live in areas exposed to levels of particulate matter (PM) higher than those recommended by WHO (Gouveia et al., 2021). The most dangerous sources of pollution relate to anthropogenic activities, such as industrial waste management, vehicles, and house heating (Park et al., 2018). One of the most hazardous pollutant dispersed in the air is the PM, which consists of a heterogeneous combination of organic and inorganic elements in different states. Its dangerousness is connected with the risk to human health since it causes serious problems, mainly associated with respiratory diseases (Guo et al., 2022; Li et al., 2019; Schraufnagel et al., 2019; Yu et al., 2016). This is especially true for the fine particles (PM_F), which can penetrate deeper into the respiratory system compared to large and coarse particles (PM_L and PM_C)(Pryor et al., 2022). For this reason, PM was included in carcinogenicity Group 1 by the IARC (International Agency for Research on Cancer, https://www.iarc.who.int/) (Loomis et al., 2013).

Plants can significantly reduce air concentrations of pollutants by capturing particles on leaf surfaces (Abhijith et al., 2017; He et al., 2020). The use of trees for phytoremediation of air pollution has been widely investigated thanks to the plant ability to accumulate dust particles on the leaf surface. The composition of PM in terms of heavy metals has been determined in different plant species that showed a different capability to withhold PMs (Kończak et al., 2021). Green roofs with vegetation of different plant types (shrubs, trees, herbaceous species) showed to efficiently reduce air pollutants and they can be used to implement on existing, retrofitted or new buildings (Gourdji, 2018). Green barrier species showed to improve air quality through PM capture. The availability of different plant species in a green barrier is beneficial to use different mechanisms for particulate matter adsorption

* Corresponding author at: Department of Biology, University of Florence, 50019 Sesto Fiorentino, Italy.
E-mail address: federico.martinelli@unifi.it (F. Martinelli).
[1] These authors equally contribute

https://doi.org/10.1016/j.envexpbot.2023.105313
Received 17 December 2022; Received in revised form 4 March 2023; Accepted 23 March 2023
Available online 27 March 2023

due to the expanded range of leaf micromorphological differences (Redondo-Bermúdez et al., 2021).

Indeed, garden plants and shrubs can be a powerful system acting as a natural filter against pollution (Kovacs et al., 2022; Luo et al., 2019). However, not all plants have the same absorption potential for all types of pollutants. The deposition and penetration of the substances depends on the plant's phenotypic characteristics, such as the leaf area and the presence of shoot structures and on the characteristics of the polluting particles and the environment (Mori et al., 2018). Therefore, the remediating action of plants is influenced by a series of factors that make it difficult to univocally identify a valid way of action for air purification. Moreover, plant height is a fundamental trait to be considered: the plants should be higher than the atmospheric layer in which dust is concentrated to impact easily with the particles (Zhou et al., 2022). Nonetheless, it is necessary to maintain a compromise between the size of the plants and the road surface available. For this, shrubs and trees are the most suitable to retain PMs along traffic road streets (Popek et al., 2022; Prigioniero et al., 2022). Another important factor affecting plant capability to reduce air particulate matter is connected with the vegetative cycle of the plants considered for remediation: evergreen ones are the most suitable to reduce air dust that is typically higher in winter than in summer (Pikridas et al., 2013).

Moreover, also microbes and plant microbiota may contribute to air pollution remediation through their metabolic activities, degrading the pollutants, or by increasing plant growth and tolerance to abiotic stress (Espenshade et al., 2019; Syranidou et al., 2018). The phyllosphere indeed is composed of 10^6-10^7 microbial cells/cm^2 colonizing the leaf surfaces, despite the adverse environment characterized by uneven conditions. Since plants live in intimate association with diverse bacteria, these microorganisms have evolved genes that enable them to adapt to plant environments (Levy et al., 2018). However, while the interaction between plants and microbes has been extensively documented as a source of phytoremediation, the available literature concerning phylloremediation is still poor (Wei et al., 2017). Indeed, to date, various studies have focused on the role of plant roots or canopy as air depurators (Gawronski et al., 2017 and references therein), but few of these pointed out the interaction between plants and their microbiota (Sillen et al., 2020). Furthermore, there are scarce evidence relating to a modification of the phyllosphere, or in general the leaf microbiota, including both epiphytic and endophytic bacteria, in polluted areas compared to rural environments.

To our knowledge, there are no studies on the effects of air PM on leaf microbiota. *Photinia* x *fraseri* L. belongs to the Rosaceae family, which is considered the third most economically relevant plant family (Dirlewanger et al., 2004). It is an ornamental shrub that grows up to 3–5 m in height and is common in urban green areas under 1000 m of altitudes (Li, 2021). The colour of its leaves migrate from the bright red of the younger ones to the dark green of the older ones (Larraburu et al., 2010). The tolerance of *P.* x *fraseri* to pruning and air pollution makes it widely used for roadside hedges thus reducing atmospheric contamination caused by anthropogenic activities in urban areas during the whole year and especially in the winter, the most polluted season. Several studies, in particular, reported the efficiency of *P.* x *fraseri* in the adsorption of particulate matter (PM) and elements (including heavy metals) due to its phenotypical traits, especially concerning the leaf size (Fang et al., 2021; Mori et al., 2018).

In this work, we investigated how different exposure to PM may affect the leaf transcriptome and microbiome. PM accumulation data were compared with transcriptomic analyses to shed light on the plant molecular mechanisms that are affected by the adsorption of PM by the leaves. Moreover, we characterized the leaf microbiota of the same *P. x fraseri* plants to investigate on the possible effect of PMs on plant-associate microorganisms.

2. Material and methods

2.1. Experimental trial

The experiment was carried out in two areas in Altopascio (Lucca, Tuscany, Italy), characterized by different anthropogenic pressures in relation to air pollution based on PMs. A rural area was chosen as control (less increase of PMs) and compared to a main road area, characterized by intense vehicular traffic (high increase of PMs). The air levels of PMs (μg/m3) together with other environmental parameters (air temperature, relative humidity, CO_2, O_3, NO_2, CO, Total VOC) for both areas were determined using Airquino (https://www.airqino.it/), an instrument developed by the National Research Council of Italy (CNR). 10 Plants of *Photinia* x *fraseri* L. were planted in pots using commercial soil; they had a height of around 1.5 m. Plants were divided in two groups: 5 plants were cultivated in a rural area (named "R"; less levels of PM) sparsely inhabited used as a control, and 5 plants were planted in an area extremely involved in urban traffic (named "T"; higher level of PM) and therefore highly polluted by PMs. Plants were irrigated once every week and they were routinely checked to determine if any symptoms of biotic and abiotic stresses occurred. Healthy, fully-expanded, green leaves were sampled from the 5 plants from each zone at the time of planting (T0; 16th March 2021) and three months after planting (T1; 22th June 2021). Plants remained healthy during the three months of the experimental trial. Leaves were immediately frozen in liquid nitrogen and stored at – 80 °C until RNA extraction.

2.2. PM analysis and morphological analysis

The filtration methodology was performed according to Dzierżanowski et al. (2011) using three filters with different retention capacities (retention 10 μm, retention 2.5 μm, and PTFE membrane - retention 0.2 μm). Each filter was dried at 60 °C for 30 min and then left for 60 min at a constant relative air humidity (50%) for weight stabilization and then pre-weighed. Each leaf sample was washed for 60 s with 150 ml of deionized water under agitation. The washing solution was then sequentially filtered using the three filters. Filtration was carried out using an apparatus equipped with a 47 mm glass filter funnel connected to a vacuum pump. After filtration, filters were dried, left to stabilize, and weighed again. At the end of the filtration procedure, particles of different sizes were divided as large: > 10 μm (PM_L), coarse: 2.5–10 μm (PMc), fine: 0.2–2.5 μm (PM_F), and PM_T = Total sum of PM_L+PM_C+PM_F. Two-Way ANOVA was applied considering the effect of Area (R and T) and Time (T0 and T1) in the accumulation of PM_T, divided by the particle size and leaf traits. In addition, principal component analysis (PCA) was performed to group the PM_T accumulated on the leaves.

2.3. Transcriptomic analysis

RNA-seq analyses were carried out for a total of 16 samples. In particular, for each location (R and T), a pool of mature leaves was collected from 4 plants at each time point (T0 and T1). Frozen leaves were grounded in liquid nitrogen and a CTAB-modified protocol was used (Doyle and Doyle, 1987) to extract RNA from the tissue powder. The RNA obtained from each sample and eluted in nuclease-free water, was treated with DNaseI (NEB) and purified using specific silica-based columns (Monarch RNA Cleanup kit – NEB). Agilent 2100 Bioanalyzer (kit RNA nano - Agilent Technologies) and Qubit™ 4 Fluorometer (kit RNA BR - Thermo Fisher Scientific) were used to respectively check the quality and quantity of the nucleic acid extracted. Each sample was converted into sequencing libraries following the procedure of Stranded mRNA Library Prep (Illumina) and a combination of exclusive unique dual index. The concentration of each of the libraries was determined using Qubit™ 4 Fluorometer (dsDNA High Sensitivity Kit - Invitrogen). Sequencing was performed using Novaseq 6000 SP Reagent Kit (2 ×100

+ 10 + 10 bp parameters).

2.4. Transcriptome assembly and RNA-Seq data elaborations

The RNA-Seq raw reads data in fastq format were obtained from BCL files using bcl2fastq2 v2.20 (Illumina), and the quality of sequenced libraries was evaluated using FastQC v0.11.5 (Andrews, 2010). Adaptors sequences and low quality bases were removed using Trimmomatic v0.39 (Bolger et al., 2014) with these parameters: HEADCROP:1 LEADING:3 TRAILING:3 SLIDINGWINDOW:4:18 MINLEN:40. The filtered reads of the RNA libraries were *de novo* assembled with Trinity v2.13.2 (Grabherr et al., 2011), and the assembled transcripts were clustered using CD-hit v4.7 (Fu et al., 2012) with default parameters to produce a set of 'non-redundant' representative sequences for *Photinia* transcriptome. *De novo* assembled and clustered transcriptome statistics were obtained using 'n50' Perl script (https://metacpan.org/pod/distribution/Proch-N50/bin/n50), while BUSCO v5.3.2 (Simao et al., 2015) with the 'viridiplantae_odb10' lineage dataset was used to assess the completeness of the transcriptome. Pairwise sequence comparison of the predicted assembled transcripts was performed using the BLAST+ blastx-fast algorithm (Camacho et al., 2009) through the Galaxy platform (Afgan et al., 2018) against the SwissProt and Araport11 protein databases, using an expectation value cutoff of 1e-6.

The filtered RNA reads of the sixteen *Photinia x fraseri* RNA-Seq libraries were mapped to the assembled and clustered *Photinia* transcriptome, and the quantification of each transcript was carried out with the utility "align_and_estimate_abundance.pl" of Trinity v2.13.2 (Grabherr et al., 2011) using the Bowtie aligning method. The raw counts of reads mapped to each transcript were normalized basing on the reads of each library, and not expressed or poorly expressed transcripts (a transcript was considered 'active' if CPM (counts per million mapped reads) was > 1 in at least three libraries) were filtered out. Afterwards, Bioconductor EdgeR v3.38.1 (Robinson et al., 2010) with likelihood test were used to do the DE (differentially expression) analysis for three transcriptome pairwise comparisons (Rural at time 1 *Vs.* Rural at time 0; Traffic at time 1 *Vs.* Traffic at time 0; Traffic at time 1 *Vs.* Rural at time 1). Transcripts with a resulting false discovery rate (FDR) lower than 0.05 and a $\log_2$ fold change (LFC) lower than -1 or higher than 1 were considered differentially expressed transcripts (DETs).

The Blast2GO software suite v5.2 (https://www.blast2go.com/) was used to perform homology searches (BLASTX and BLASTN) with Gene Ontology terms for unique sequence and functional annotation (GO; http://www.geneontology.org/), protein sequence analysis and classification (InterPro, EBI, https://www.ebi.ac.uk/interpro/). Sequences were blasted against a nonredundant (nr) protein database that corresponds to the National Center for Biotechnology Information (NCBI, https://www.ncbi.nlm.nih.gov/) via BLASTx-fast. InterPro was performed in parallel with the blasting phase, followed by the Gene Ontology mapping and gene annotation. Subsequently, the Gene Ontology terms that were derived from the BLAST and InterPro steps were merged. Go-slim reduction was applied. BLAST2GO was also used for assigning the genes to cellular processes, biological functions, and cellular components, as well as other salutary statistics. Hierarchical clustering and QT-clust analysis of data, based on the three values attributed, was carried out using MeV v4.6.2 software (http://www.tm4.org/).

2.4.1. Identification of Arabidopsis orthologs

Transcripts resulting from the assembly and clustering operations were aligned to *Arabidopsis thaliana* L. reference transcriptome using BlastX against Araport11 dataset (Cheng et al., 2017) with an e-value cutoff of 0.001 through the Galaxy Europe toolkit (Afgan et al., 2018); https://usegalaxy.eu/). For each transcript, the best BlastX hit was considered as the Arabidopsis putative orthologue. In order to correctly evaluate the transcripts expression levels basing on Arabidopsis ortholog, the reads counts of Photinia transcripts having the same Arabidopsis putative orthologue were summed for the sixteen RNA libraries. Then, the resulting summed raw counts were normalized, filtered and used for DE analyses with the same methods described on 2.4 paragraph. Transcripts with a resulting false discovery rate (FDR) lower than 0.05 and a $\log_2$ fold change (LFC) lower than -5 or higher than 5 were considered as differentially expressed.

2.5. Functional data mining and enrichment analyses

According to the DE analyses results, functional data mining was performed analyzing the pairwise comparisons of DETs between T1 and T0 for each location (Traffic, T1 vs T0; Rural, R1 vs R0). The pairwise comparison at T1 between Traffic and Rural was also conducted (T1 vs R1). Common and exclusive DETs between the two different locations comparing different time points were determined to dissect the complex gene regulatory networks underlying plant responses to different air particulate matter concentrations in the two analyzed close-by areas. Principal components were calculated using one of the methods in pcaMethods R (Stacklies et al., 2007) with the Nipals package. PCA iteratively finds components by leaving out missing values when calculating inner products. Vector scaling methods were used to data pre-processing which divides the values by the Euclidean norm of the values (square root of sum of squared values). The gene visualization in biological pathways was performed using MapMan 3.6.0RC1 software (http://mapman.gabipd.org/) to identify and visualize genes in functional overviews of cell pathways and gene categories (Thimm et al., 2004). The gene set enrichment analysis using Pageman was carried out with the same list of DE genes (http://mapman.gabipd.org/). The analysis was performed through the Wilcoxon test without correction and with a cutoff value of 1. The Database for Annotation, Visualization, and Integrated Discovery (DAVID) v.6.8 (https://david.ncifcrf.gov/) (Dennis et al., 2003) was used to get the gene ontology information related to the biological processes regulated by environmental stresses. STRING v.11 web-tool was used to visualize the gene-gene interaction network among the commonly regulated genes (https://string-db.org/), setting a confident score cutoff = 0.9 (Szklarczyk et al., 2018).

2.6. Taxonomic characterization of leaf microbiota

Total DNA was extracted by leaf tissues using CTAB-modified method from the same samples collected for transcriptomic analysis (Doyle and Doyle, 1987). Indeed, microbiome analysis were conducted at same time points of RNA-seq analysis: at the beginning (T0 and R0) and after 3 months from the beginning of the trial (T1 or R1). The V3-V4 region of the bacterial 16 S rRNA gene was amplified as previously reported (Cangioli et al., 2022), while fungal internal transcribed spacer 1 (ITS1) was amplified (Almario et al., 2022). Libraries were constructed following the Illumina 16 S Metagenomic Sequencing Library Preparation protocol and sequenced on MiSeq instrument (Illumina, San Diego, CA) using 300-bp paired-end cycles. Library preparation (Nextera XT, Illumina, San Diego, CA, USA) and sequencing (MiSeq Reagent Kit v3, Illumina, San Diego, CA, USA) were conducted at IGA Technology Services (Udine, Italy). Demultiplexing was performed following Illumina's standard pipeline, as previously reported (Cangioli et al., 2022). Data analysis was performed as previously reported (Cangioli et al., 2022). In brief, DADA2 pipeline (version 1.24.0) (Callahan et al., 2016) was used to cluster amplicon sequence variants (ASVs). Both ASV reconstruction and statistical analyses were performed in the R environment version 4.2.0 (http://www.R-project.org). After filtering, trimming, dereplicating, merging and chimera removal, the bacterial taxonomy assignment was carried out comparing 16 S rRNA ASV against SILVA_SSU_r138 database (Quast et al., 2013) using "DECIPHER" R package (version 2.24.1) (Wright et al., 2012) as implementation of DADA2 (SSU version 138 available at: http://www2.decipher.codes/Downloads.html). Annotated ASVs count tables were processed in Phyloseq package (McMurdie and Holmes, 2013). All sequences classified as chloroplasts,

mitochondria, Archaea and Eukarya were removed.

For ITS reads, after assigning to ASV using DADA2 taxonomy assignment was carried out on the UNITE ITS database (Nilsson et al., 2018), using a native implementation of the naive Bayesian classifier method for taxonomic assignment provided by DADA2 package (UNITE_v2020_February2020 version available at http://www2.decipher.codes/Downloads.html). The "assignTaxonomy()" function was used. Alpha diversity (Shannon and Pielou's Evenness indices) were calculated using the function "diversity()" within "Phyloseq" R package (Nilsson et al., 2018). Good's coverage and evenness indices were calculated through the R functions 'goods()' and 'evenness()', respectively, within the 'microbiome' R package (version 1.12.0). Taxonomic differences among microbiota were inspected by non-metric multidimensional scaling (nMDS), using the "ordinate" function and plotting by the "plot_ordination()" function within phyloseq package. Rarefaction curves were generated using the "ggplot2" (version 3.3.6) (Villanueva and Chen, 2019) and "ranacapa" (version 0.1.0) (Kandlikar et al., 2018) R packages using the "ggrare()" function on the phyloseq object. The "ggplot2" R package (version 3.3.6) was used to generate relative abundance plots. Different community structures were analyzed using permutational a multivariate analysis of variance (PERMANOVA) using the R packages "vegan" (version 2.6.2) and the function "adonis2()".

Differential abundance analysis was performed using the R package DESeq2 (version 1.36.0) (Love et al., 2014).

2.7. qRT-PCR analysis

The RNA samples were treated with RNase-free RQ1 DNase I (Promega) and used for cDNA synthesis using oligo-$(dT)_{20}$ primer and SuperScript III RT mix (Life Technologies, Carlsbad, CA, USA). The cDNA samples were diluted 1:10 (v:v) with nuclease-free water, while the real-time PCR assays were performed in QuantStudio 7 Flex Real-Time PCR System (Applied Biosystems, Waltham, MA, USA) using 3 μL cDNA, 0.1 μM gene-specific primers (Table Supplementary 1), and SYBR Green PCR Master Mix (Applied Biosystems). The relative gene expression was calculated with the $2^{-\Delta CT}$ (Livak and Schmittgen, 2001) and $2^{-\Delta\Delta CT}$ (Rao et al., 2013) formula using DN4017_c0_g1_i1 (THF), and DN34523_c0_g1_i3 (TMp1) as endogenous reference genes (Table Supplementary 1). These three reference genes were previously validated in apple tree (Perini et al., 2014) and their sequences were used to search for orthologous genes in Photinia. Four biological replicates for each treatment were used. All cDNA samples were carried out in technical triplicate reactions. The target-specific amplification was confirmed by the occurrence of a single peak in the melting curve.

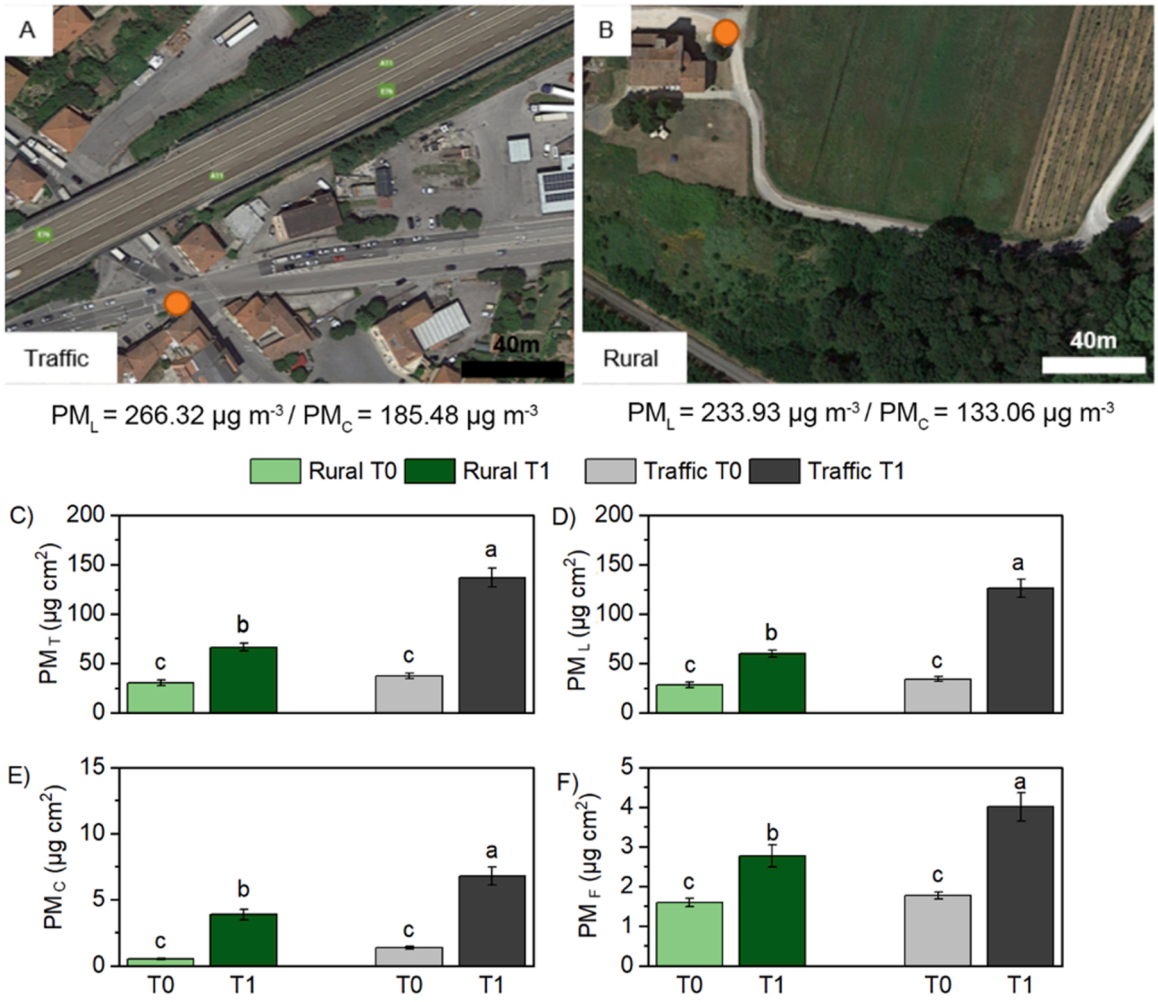

Fig. 1. A) Traffic area and B) Rural area with the accumulated PM_L and PM_C registered 22 day before the end of the experimental period. C-F) PM divided by the particle size accumulated in *Photinia* leaves collected from two different areas of study (Traffic and Rural) at two different times (T0 and T1) during the summer season 2021. C) PM_T = Total sum of PM_L+PM_C+PM_F; D) Large = PM_L > 10 μm; E) Coarse = PM_C. 2.5–10 μm and F) Fine= PM_F 0.2–2.5 μm. Letters represent differences between areas and time (Tukey test, $p < 0.05$).

3. Results

3.1. PM accumulation in leaves

During the exposure period the average temperature were 15 °C (min 10 °C, max 21 °C), the relative humidity was 70% (45 – 96%) and the wind of 3.5 km/h (0.5 – 11.3 km/h) was prevalently West-Southwest (© Meteo System | Osservatorio Meteorologico di Lucca - Zona Arancio, Toscana – Italia).

The last precipitation above 10 mm was recorded 22 days before the end of the experimental period and the accumulation of PM_{10} and $PM_{2.5}$ was higher in T (Fig. 1 A) compared to the R area (Fig. 1B). An interaction between time and area factors was verified for all the PM fractions analyzed (Table 1). For all assessed particle fractions, the time point 1 (3 months after the beginning) presented higher values than time point 0 (beginning of the trial) either for Rural or Traffic areas (Fig. 1 C-F). Furthermore, the T1 presented higher values than the R1 for all parameters (Fig. 1 C-F). Indeed, these data showed that also in rural conditions a significant increase of PMs was observed and this region could not be considered as pollution-free. However, this increase was lower than in traffic conditions so the comparison of plant responses between the two locations is possible and useful to highlight different gene regulatory responses to air PM levels.

3.2. RNA sequencing and de novo transcriptome assembling

Overall, the number of resulting paired raw reads for each library ranged from 18 to 31 million, for a total of 343.1 million (Table 2). Percentage of reads 'survived' to filtering ranged from 92% to 95% (Table 2).

3.3. Venn diagrams and GO-term enrichment analysis of pairwise comparisons

Venn diagrams were constructed to determine the number of DETs unique and in common between the pairwise comparisons of different time points at the same location and of different areas at three months after the beginning of the trial (R1 vs R0, T1 vs T0 and T1 vs R1 - Fig. 2A). A total of 8242 differentially expressed transcripts were analyzed using BLAST2GO. Among them, 59 genes were in common between the three pairwise comparisons (R1 vs R0, T1 vs T0, T1 vs R1), 2866 genes in common between R1 vs R0 and T1 vs T0 conditions, 785 genes in common between R1 vs R0 and T1 vs R1, 124 in common between T1 vs T0 and T1 vs R1 and 74, 2043 and 2294 unique respectively to R1 vs R0, T1 vs T0 and T1 vs R1 (Table Supplementary 2, Table Supplementary 3, Table Supplementary 4). The most probable *Arabidopsis* orthologue for each transcript was searched, and 22,584 *Arabidopsis* proteins were found to have at least one orthologue in the *Photinia* assembled transcriptome (Table Supplementary 5). Differential expression analyses have been carried out considering the summed counts for each orthologue Arabidopsis transcript, and the resulting DETs were 2676 for R1 vs R0 comparison (1180 down-regulated; 1496 up-regulated), 2696 for T1 vs T0 comparison (1203 down-regulated; 1493 up-regulated) and 367 for T1 vs R1 comparison (312 down-regulated; 55 up-regulated) (Fig. 2B). Detailed DE analyses results are reported in Table Supplementary 5.

Table 1
A) Results of the Two-Way ANOVA considering the effect of Time (T0 and T1) and Area (Traffic and Rural) in the accumulation of particulate matters (PMs), divided by the particle size, in *P. fraseri* leaves collected. B) Results of the Two-Way ANOVA considering the effect of Time (T0 and T1) and Area (Traffic and Rural) in the leaf traits analyzed: Leaf surface area (LA in cm^2); leaf roundness (LR); specific leaf area (SLA in $m^2\ kg^{-1}$) and leaf dissection index (LDI).

	Effect	PM_L	PM_C	PM_F	PM_T
A)	Time	* **	* *[a]	* **	* **
	Area	* **	* **	* *	* **
	Time*Area	* **	*	*	* **
		LA	LR	SLA	LDI
B)	Time	n.s	n.s	n.s	n.s
	Area	n.s	n.s	n.s	n.s
	Time*Area	n.s	n.s	*	n.s

[a] = $p < 0.05$, * * = $p < 0.001$, * ** = $p < 0.001$, n.s = non significant

Table 2
For each RNA library, the number of raw reads pairs and number and percentage of survived reads after filtering were reported.

RNA library	Condition	Time-point	Raw read pairs (#)	Read pairs survived to filtering (#)	Read pairs survived to filtering (%)
R0_1	rural area	0	19,466,329	18,181,545	93.40%
R0_2	rural area	0	31,079,586	28,791,118	92.64%
R0_3	rural area	0	20,312,641	18,895,568	93.02%
R0_4	rural area	0	20,589,680	19,517,672	94.79%
R1_1	rural area	1	23,406,485	21,709,176	92.75%
R1_2	rural area	1	19,193,945	17,882,154	93.17%
R1_3	rural area	1	23,377,567	21,843,427	93.44%
R1_4	rural area	1	18,139,659	16,856,104	92.92%
T0_1	traffic	0	23,543,118	22,009,812	93.49%
T0_2	traffic	0	23,510,851	21,774,720	92.62%
T0_3	traffic	0	18,742,202	17,573,312	93.76%
T0_4	traffic	0	21,543,579	20,192,772	93.73%
T1_1	traffic	1	20,660,840	19,477,537	94.27%
T1_2	traffic	1	20,836,477	19,281,245	92.54%
T1_3	traffic	1	18,658,024	17,511,100	93.85%
T1_4	traffic	1	20,049,766	18,841,008	93.97%

3.4. Principal component analysis of RNA-seq

A MDS (Multi-Dimensional Scaling) chart was performed to determine the "general" differences between sampling area and time points (Figure S.1). The two different time points were clearly separated through the dimension 1 while a separation was less evident (but present) between the two experimental sites. The PCA analysis carried out on all the different groups of the common DETs (Fig. 3) showed that R1 and T1 conditions were clearly discriminated from the T0 and R0. Indeed, these 59 genes in common between the three experimental conditions (R1 vs R0, T1 vs T0 and R1vs T1) (Fig. 3A) highlighted that DETs of T1 and R1 conditions clustered very near and clearly separated from the T0 and R0 ones. The PCA analysis of the 124 genes (Fig. 3B) in common between T1 vs T0 and T1 vs R1 showed that T1 and R1 condition clustered clearly separated. The PCA of the 785 genes in common between R1 vs R0 and T1 vs R1 (Fig. 3 C) showed that R1 condition was clearly different from the other three groups (T0, R0 and T1). Finally, the PCA of 2866 genes in common to R1vs R0 and T1 vs T0 (Fig. 3 D) showed a clear separation between the two timepoints while the two areas were similar.

3.5. Phylogenetic analysis, co-expression and sequence comparisons

The co-expression analysis of the 59 DETs in common between the

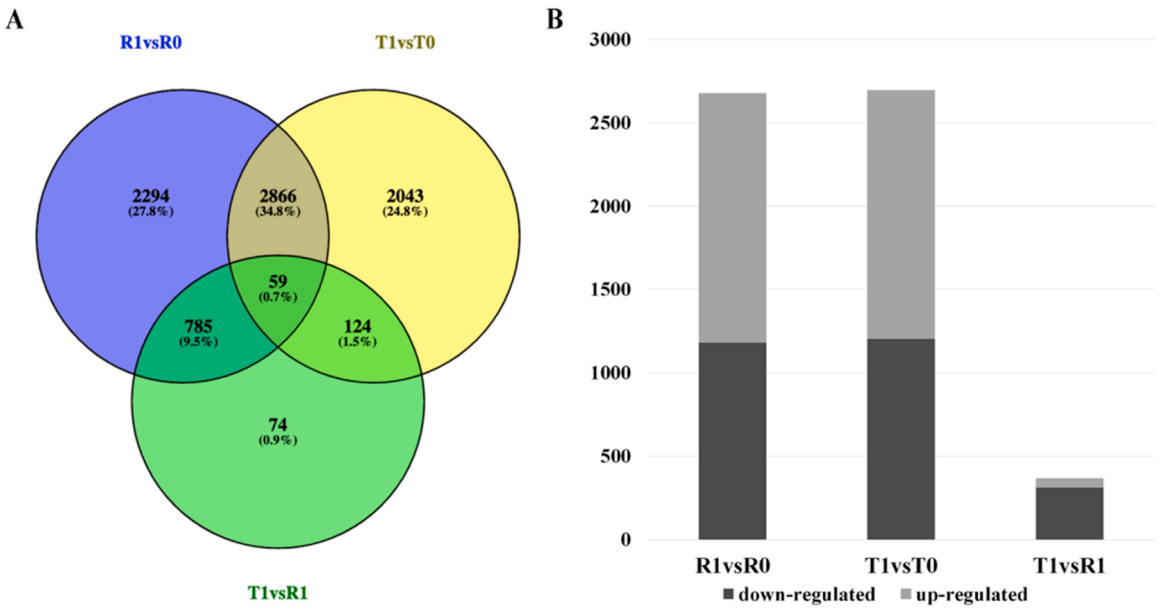

Fig. 2. A) Venn diagram of differentially expressed transcripts for each pairwise comparisons: R1 vs R0, T1 vs T0 and T1 vs R1 conditions. The number of genes in common between the three pairwise comparisons were also shown. The percentage of genes for sub-groups of commonly and uniquely expressed genes was also indicated. B) number of down- and up-regulated transcripts with Arabidopsis orthologs for R1 vs R0, T1 vs T0 and T1 vs R1 comparisons.

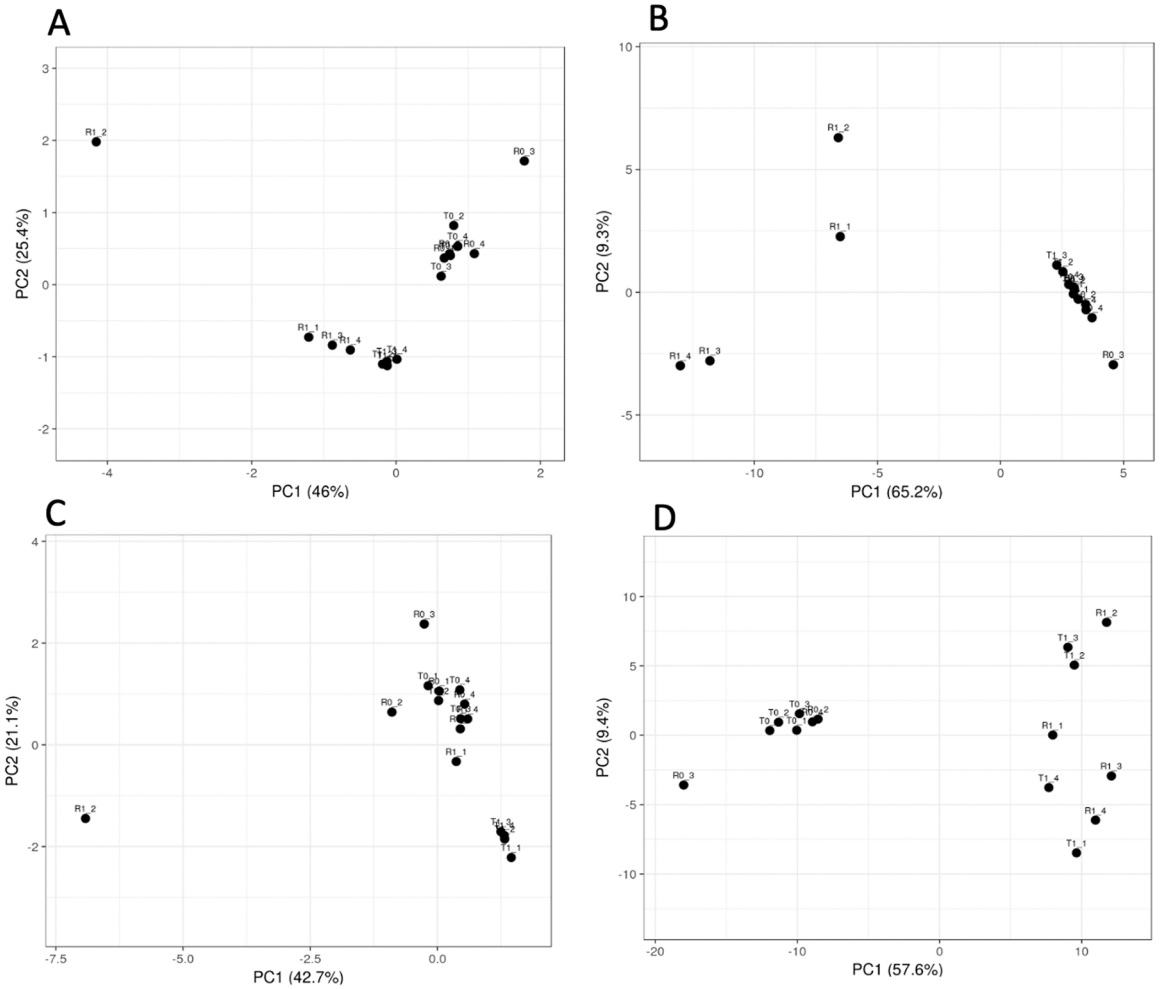

Fig. 3. The principal component analysis (PCA) of different groups of common genes: A) 59 genes common to the three pairwise comparisons R1 vs R0, T1 vs T0 and R1 vs T1), B) 124 genes in common between T1 vs T0 and T1 vs R1, C) 785 genes in common between R1 vs R0 and T1 vs R1 and D) 2866 genes in common between R1 vs R0 and T1 vs T0.

three pairwise comparison showed that inside this group there were 3 clusters of genes that were differently modulated inside the T1 vs T0, R1 vs R0 and T1 vs R1 conditions (Figure S.2). These results were confirmed when the same group of genes were analyzed using the QT-CLUST tool. According to this analysis, 28 genes were upregulated in R1 vs R0 and repressed in the other two comparisons (Figure S.3, cluster 1) highlighting that these genes should be the most affected by air particulate matter. They represent a signature of plant responses to air pollution at transcript level. Indeed, they distinguished the rural and traffic conditions since all these genes were repressed by higher level of pollution while upregulated in rural condition. Among them it is worth mentioning some genes involved in ribosome assembly, peptide biosynthetic process and also amide biosynthetic processes. On the other hand, 19 genes showed to be upregulated in T1 vs R1 while it was repressed in R1 vs R0 and T1 vs T0 (Figure S.3, cluster 2). They belonged to three main categories: xanthophyll metabolic process, tetraterpenoid metabolism and carotenoid metabolism (Table Supplementary 6).

Cluster 3, cluster 4, cluster 5 and cluster 6 (Figure S.3) were characterized by set of genes that were mainly downregulated in all the experimental condition including genes involved in cell wall metabolism such as *beta-glucuronidase*, *omega-3 fatty acid desaturase*, *cinnamyl-alcohol dehydrogenase*, *sinapyl alcohol dehydrogenase* (Table Supplementary 6).

The co-expression analysis of the 785 DETs in common between T1 vs R1 and R1 vs R0 showed that 600 genes were upregulated in R1 vs R0 and repressed in T1 vs R1 (Figure S.3, cluster 7). Several gene categories were highly represented such as ribosome assembly, protein folding or peptide biosynthetic process. At the same time, 185 genes have an opposite trend: repressed in R1 vs R0 and upregulated in T1 vs R1 (Figure S.3, cluster 8) and the most represented gene category was ATP-dependent activity (Table Supplementary 6).

Cluster 9 and Cluster 10 (Figure S.3) were composed by genes with a very similar trend of expression in all the three pairwise comparisons. Most of them belonged to the following categories: response to reactive oxygen species, oxidative stress and temperature stimulus (Table Supplementary 6).

3.6. Gene set enrichment analysis

The gene set enrichment analysis highlighted that some gene categories of the primary metabolism were significantly upregulated in R and not in T such as fermentation, TCA, mitochondrial electron transport /ATP synthesis (Fig. 4). Gluconeogenesis was inhibited in T while induced in R. On the other hand, cell wall precursor synthesis was downregulated in T, while some lipid-related genes (*FA synthesis* and *FA elongation*) were regulated similarly in the two conditions, others showed extremely different pattern of expression (*FA desaturation desaturase* and *lysophospholipases carboxylesterase*). Pathways involved in nitrogen and amino acids metabolism were significantly regulated (up- or down-regulated) in the rural context while they were unmodulated in plants subjected to higher pollution concentration (Fig. 4). Several interesting pathways were significantly affected by different PM concentrations. They belonged to secondary metabolism such as lignin, flavonoids and phenols. In the traffic area genes involved in abscisic acid and gibberellins metabolism were upregulated while they were not regulated in the rural counterpart, where it was mainly observed a trend of down-regulation in cytokinin metabolism. Although both conditions showed an induction of stress categories, this was more pronounced in T area. Relating to the transcriptional regulation, rural area showed more differentially regulated genes than traffic area. This was confirmed also for genes involved in general pathways of the protein metabolism. Finally, the transport categories (sugars, sulphates and metals) were down-regulated in T and not in R.

3.7. Metabolic pathways and gene categories

Differentially expressed genes in the two pairwise comparisons (T1 vs T0 and R1 vs R0) involved in metabolism overview were shown in Fig. 5. Most of the genes showed a similar trend of expression between the two pairwise comparisons. At the same time, genes such as *sugar isomerase* (*SIS*) *domain-containing protein*, *AtGolS2* and *Gsl03* both involved in minor CHO metabolism and genes like *Exp1* and *Exp8* involved in cell modification were downregulated in both conditions. However, some genes belonging to different categories were modulated in a contrasting way between T and R such as genes encoding *aldo/keto reductase family proteins* which were upregulated in R and downregulated in T. Genes involved in TCA cycle like *Sdh2–2* (*succinate dehydrogenase 2–2*) or *Sdh3–1* (*succinate dehydrogenase 3–1*) were upregulated in R and different genes involved in the same pathway like *Sdh1–2* (*succinate dehydrogenase*) and *Sdh2–1* (electron carrier in succinate dehydrogenase) were downregulated in T. At the same time, *Mls* (*Malate Synthase*) and *Icl* (*Isocitrate Lyase*) genes involved in gluconeogenesis were upregulated in rural condition but downregulated in traffic one. At least genes like *Fdh* (*Formate Dehydrogenase*) involved in C1-metabolism was upregulated in R and downregulated in T (Table Supplementary 6).

Two different set of genes involved in hormone biosynthesis were modulated in the two conditions analyzed (T and R) (Figure S.4). *Gasa1* (*Gast1 Protein Homolog 1*), *Gasa14* and *Gasa10* were upregulated in T conditions. Genes involved in gibberellins like *Ga20ox2* (*Gibberellin 20 Oxidase 2*) and *Gasa6* were downregulated in R conditions. Relating to auxin pathway, *Saur7* (*Small Auxin Upregulated Rna 7*) and *F28i8.9* (*Auxin-Responsive Protein-Related*) were respectively downregulated and upregulated in R conditions compared to T. *Suba4* (*Aldo-Keto Reductase Activity*), *Saur78* (*Small Auxin Upregulated Rna 78*) and *Saur1,* (*Small Auxin Upregulated Rna 1*), are a group of genes related to the same pathway modulated only in T condition (the first was upregulated and the other ones downregulated). The only difference in DETs related to brassinosteroid pathway was the *Br6ox2* (*Brassinosteroid-6-Oxidase 2*) gene, that was downregulated only in rural condition. In T condition the genes *Aoc3* involved in jasmonate metabolism was upregulated (Table Supplementary 6).

Relating to genes involved in environmental stress responses, rural condition showed a large number of downregulated genes such as protease inhibitor, *PR4* (*Pathogenesis-related 4*), *Lcr69* (*Low-molecular-weight cysteine-rich 69*) and *PR Thaumatin Family gene* (Figure S.5). Traffic condition showed a large set of upregulated genes such as *Atlptlp − 1*, *Rpp5* (*Recognition of Peronospora parasitica 5*), *RPP8-like protein 3,* a disease resistance protein (CC-NBS-LRR class), *SCP domain-containing protein* and *MSH2* that were annotated like two pathogenesis-related proteins (Figure S.5). When the air quality is higher (rural, less polluted), genes encoding heat shock proteins were more induced than in traffic conditions such as *At-hsfb2b, DNAJ heat shock family* protein, *Erd2* (*early-responsive to dehydration 2*), *17.6 kDa class I small heat shock protein* (*HSP 17.6 C-CI*), *Hsp18.2* (*Heat Shock Protein 18.2*) (Table Supplementary 7).

Among genes involved in redox reaction, some genes like *Atcxxs1*, *Apx2* (*Ascorbate Peroxidase 2*), glutaredoxin family protein and electron carrier/protein disulfide oxidoreductase followed the same trend of modulation in T and R conditions. Differently *Atpdil2–1* involved in redox reaction of thioredoxin was downregulated in T and upregulated in R. *Cb5-c* (*Cytochrome B5 Isoform C*) and *Apx5* (*Ascorbate Peroxidase 5*) involved in oxidative stress responses were upregulated in rural condition and not in traffic one (Table Supplementary 7). Genes involved in cell cycle were mostly induced in the conditions with less PM (rural) while they were not affected in the traffic area implying the air particulate has a negative effect on genes involved in cell cycle. Genes like *Atphb2* (*Prohibitin 2*), *peptidyl-prolyl cis-trans isomerase, Roc5* (*Rotamase Cyclophilin 5*) and *Rof1 (Rotamase Fkbp 1*) were upregulated only in rural condition.

In general, air particulate matter showed a higher number of upregulated genes belonging to the following transcription factor families (Fig. 6): *G2-like transcription factor family, Heat-shock transcription factor*

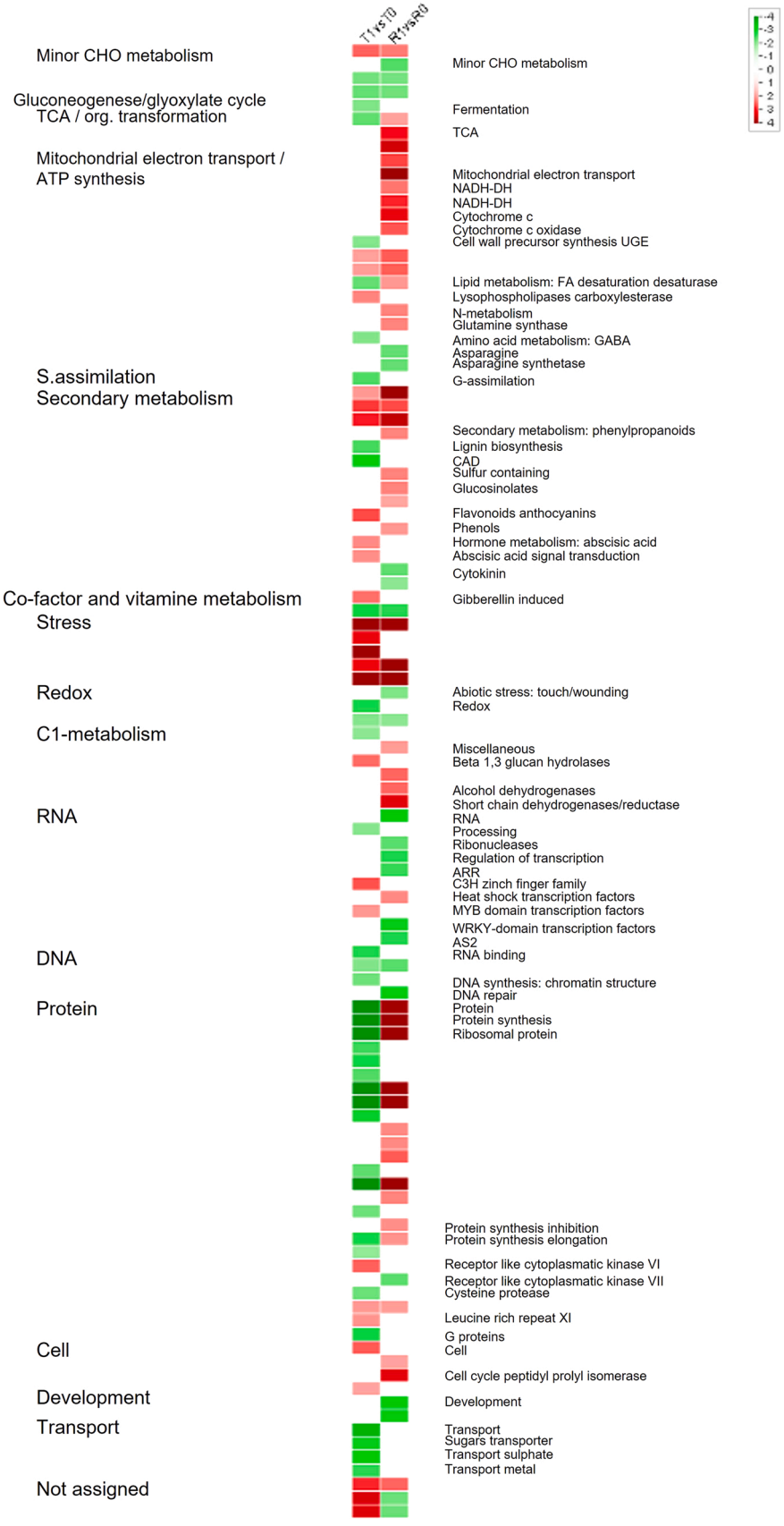

Fig. 4. Gene set enrichment categories for the pairwise comparisons using Pageman web-tool (T1 vs T0, traffic areas at two time-points; R1 vs R0, rural area). Red means upregulated while green means downregulated categories.

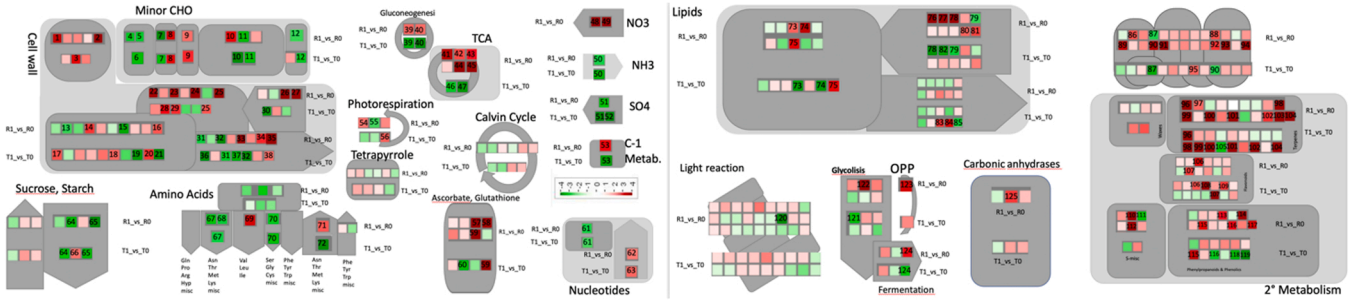

Fig. 5. Metabolism overview of differentially expressed genes in T1 vs T0 and R1 vs R0 comparisons.

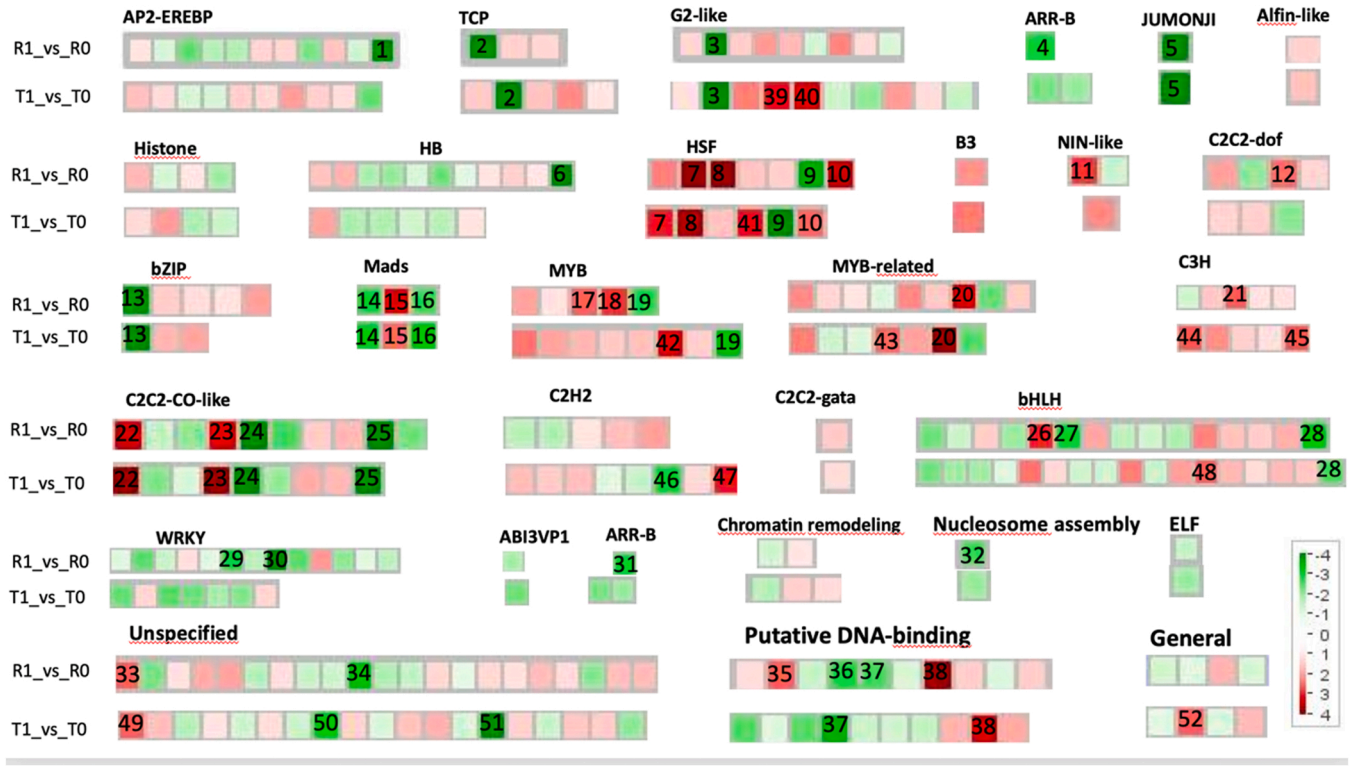

Fig. 6. Transcription factors of differentially expressed genes in T1 vs T0 and R1 vs R0 comparisons.

family, C3h zinc finger family and C2h2 zinc finger family. In addition, there were some specific genes that showed contrasting pattern of expression among the two pairwise comparisons. The following genes were repressed at higher levels of PM while they were not regulated in R: *zinc finger constans-related*, Wrky domain transcription factor family and *Zfp1* (*Zinc -Finger Protein 1*). Moreover there were some genes down-regulated in R and not regulated in T: *Wrky18, Wrky29, Arr6* (*Response Regulator 6*), *Hmgb3* (*High Mobility Group B 3*) and chloroplast nucleoid DNA-binding protein-related (Table Supplementary 8).

3.8. qRT-PCR analysis

A validation analysis using qRT-PCR was conducted for 6 genes randomly selected among different gene sets (cell wall, transcription factor, redox pathways) (Fig. S6). 5 of 6 showed the same trend of expression compared to RNA-seq data for each time point and pollution areas. Only one gene (*c-myb-like transcription factor*) was upregulated in T1 vs T0 comparison while was not modulated in the same comparison in RNA-seq analysis.

3.9. Protein-protein interaction network

Protein-protein interaction analysis, conducted using String, predicted 431 proteins encoded by DETs in common between T1 vs T0 and T1 vs R1 (Fig. 7A and B). These two comparisons were shown since they indicate genes affected by air particulate matter after 3 months. The presence of the genes in both comparisons strengthen the link between the expression of these genes and PMs air concentration. While some of them were barely interactive, others showed a high level of interactions and were very connected each other. Among these highly interactive proteins (hubs) involved in abiotic stress, it is worth mentioning different genes related to the heat shock proteins family like *HSP80* and *HSP17.9*. Among other genes showed in the networks, there were some other genes well-known to be involved in response to inorganic substance such as *PER1*, *GDH2* and *FSD2*.

3.10. Characterization of leaf microbiota

Concerning the bacterial fraction of the microbiota (viz. 16 S rRNA amplicon sequencing data), a total of 145 Amplicon Sequences Variants (ASVs) were obtained (Table Supplementary 9), 128 of which were

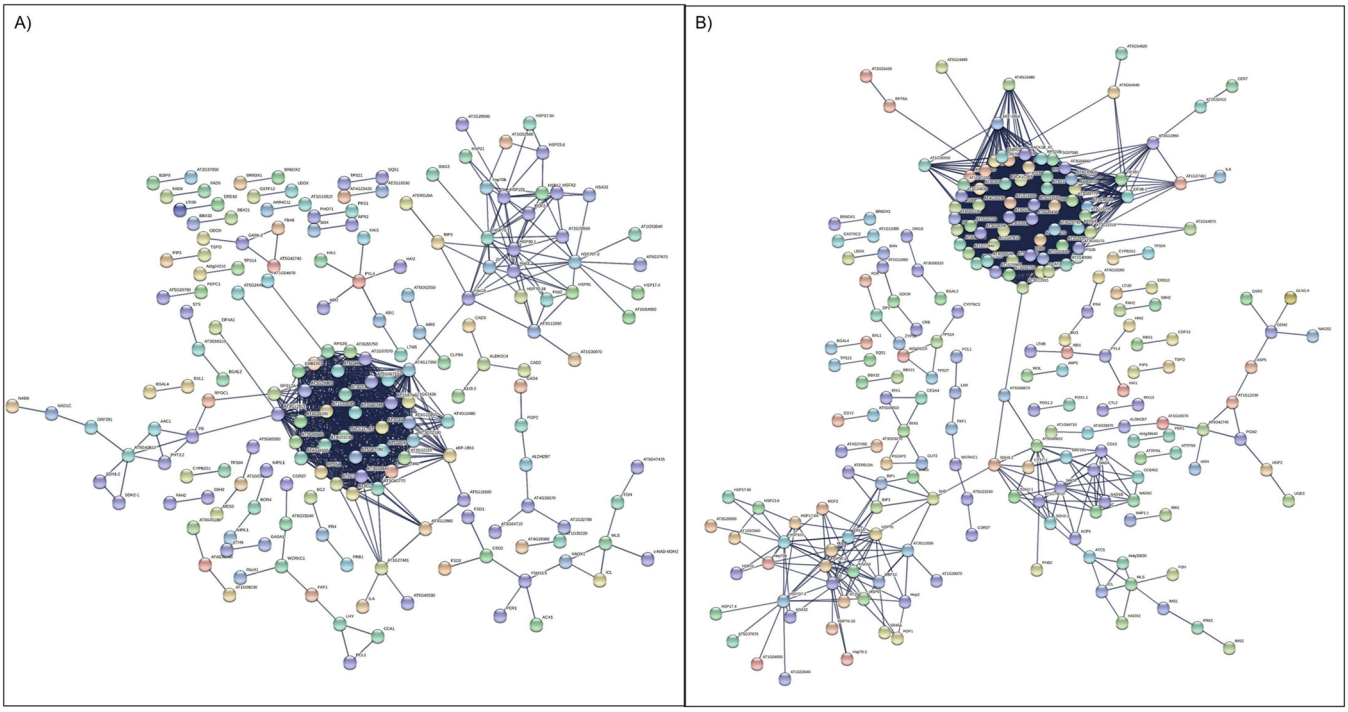

Fig. 7. Protein-protein interaction networks of DEGs found in significantly modulated GO-terms in the two pairwise comparisons. Name of key proteins with a high number of interactions were indicated. Proteins are represented by nodes while lines are predicted or experimental interactions determined using STRING software. A) Comparison between T1 and T0. B) Comparison between R1 and R0.

assigned to bacterial taxonomy. Sequences belonging to Archaea and chloroplasts, as well as ASVs not assigned (NAs), were discarded. Due to low quality of extracted DNA, the sample P10-R-T0 did not produce reads assignable to bacterial taxonomy, thus it was removed.

Good's coverage scores indicated that the sequencing depth was adequate to reliably describe the bacterial community (Table Supplementary 10). For the fungal fraction (viz. ITS amplicon sequencing data), a total of 227 Amplicon Sequences Variants (ASVs) were obtained (Table Supplementary 12). After discarding those not assigned to fungal taxonomy (NAs), 155 ASVs were considered for further analyses.

Good's coverage scores indicated a satisfactory level of sampling (Table Supplementary 13), which allowed to estimate alpha diversity indices (Table Supplementary 14).

After estimation of alpha diversity indices (Table Supplementary 11) no difference in alpha diversity values among samples from rural and urbanized area were found for the bacterial fraction (Fig. 8A). In contrast, fungal diversity showed statistically significant differences

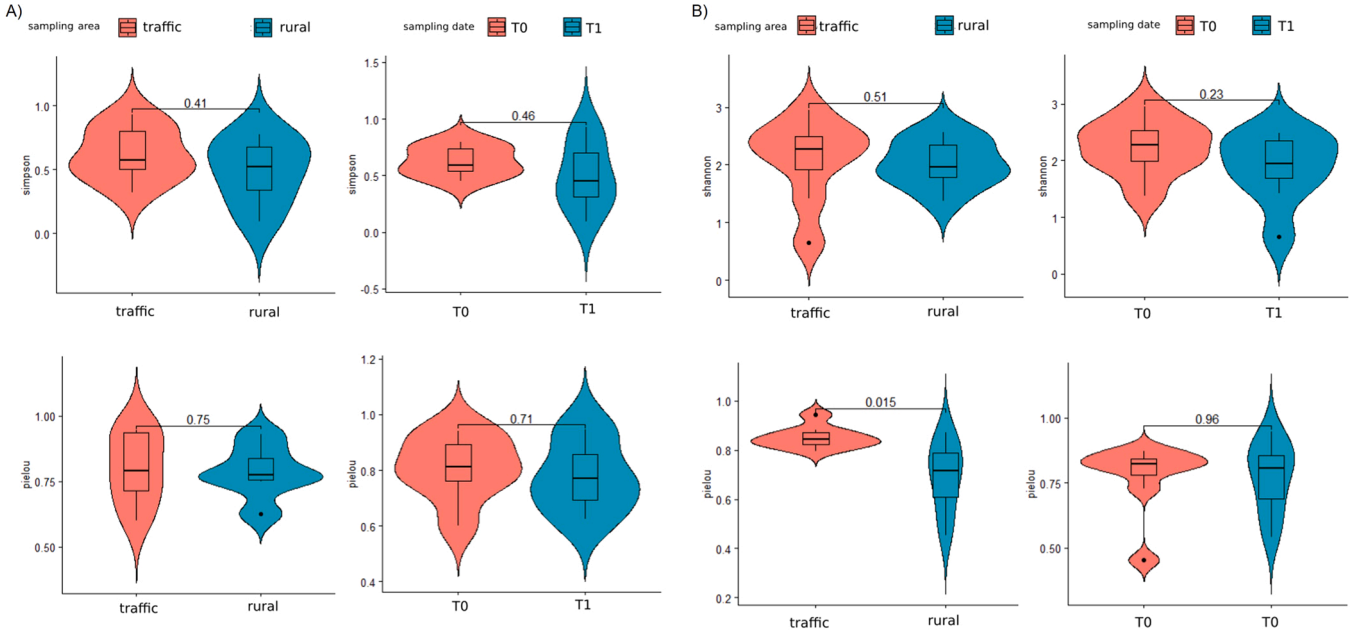

Fig. 8. Alpha diversity of bacterial (A) and fungal (B) community. Violin plots with samples are grouped according to sampling area and date. Statistical analysis was performed using Wilcoxon test (p-values are reported over the lines: not significant $p > 0.05$). The y axis indicates the values of the Pielou index and Simpson index.

between rural and urban areas for Pielou Index, indicating that evenness of fungal species changed among the two sampling areas (Fig. 8B).

In bacterial fraction of the microbiota, the most represented phyla were Bacteroidota, Proteobacteria and Firmicutes. At genus level the most abundant genera were *Pseudarcicella*, *Hymenobacter*, *Streptococcus* and *Pseudomonas* (Fig. 9A). For the fungal fraction, mycobiota were mainly composed by members of the phylum Ascomycota (Fig. 9B).

Concerning the taxonomic diversity among samples, PCA did not showed a separation between the two different areas for both bacterial and fungal communities (Fig. 10). Indeed, neither the sampling area, nor the sampling date affected the taxonomic diversity (PERMANOVA) of the bacterial fraction of the microbiota (Table 3A). However, statistically significant difference in relation to the sampling time were found for the mycobiota (fungal fraction) (Table 3B). More specifically, when we focused the attention on single ASVs instead of the total mycobiota, differential abundant analysis showed, for the fungal fraction, the presence of two ASVs showing significantly different abundance between rural and urban area. One ASV, belonging to the *Epicoccum* genus, was found increasing along time in the rural zone samples, while the other one, belonging to the *Dioszegia* genus, was decreasing along time in plants exposed to the traffic zones. Regarding the microbial fraction, one ASV belonging to *Spiroplasma* genus was found increasing along time in plants in the rural area (Table 4, Supplementary Table S15).

4. Discussion

Plant leaves are important receptors for both gaseous and PM pollutants of the atmosphere. Before these pollutants enter the leaf tissue, they interact with foliar surface and modify its configuration (Popek et al., 2018). Morphological leaf features such as hairs and waxes may enhance PM content (Jouraeva et al., 2002; Leonard et al., 2016). PM present in the leaves reduce free access of light rays to the chloroplasts ((Hirano et al., 1995). Low size PMs may clog the stomata, decreasing gas exchange (Cape et al., 2009), while chemically-active PM may influence the physiological plant processes (Chauhan, 2010). PM deposition in leaves showed an increase of various metal(loid)s in the epicuticular wax implying that PM may penetrate the cuticular barrier although they are retained on the leaf surface (Shabnam et al., 2021). In addition, immobilized fraction of PM was linked to trichome density and leaf wettability, implying that plant species with higher trichome density and/or leaf wettability accumulated more PM than plant species with less trichomes (Muhammad et al., 2020). The use of plants for the phylloremediation of air PMs in urban polluted environment is an old idea. However the molecular mechanisms underlying the capability of plants to tolerate the accumulation of PMs in leaf surfaces are completely unknown. In our study, we only observed a possible interaction of time and area with different levels of PM on specific leaf area. Although this was the only significant change between the two time points of the two areas, this parameter might be important to modulate the different levels of PMs adsorbed by leaf tissues. Considering that 1-year old plants were transplanted and leaves were already fully expanded it is expected to not observe in three months significant changes in leaf area, leaf roundness and leaf dissection index. This is due to the short time frame (3 months). The time is not enough to see morphological changes in an evergreen tree plant such as photinia. Probably this should be evident after years of PM exposition, considering the time needed by plants to acclimate to the new condition after the transplantation. The main focus of our work was to shed light on these mechanisms, and in particular on the transcriptomic changes that occur in plants exposed to higher levels of PM in comparison to plants located in a less polluted (but not pollution-free) area. At the same time, we investigated how exposure to high PM levels affects the composition of the leaf microbiota.

The PCA analysis carried out on the common DETs between three pairwise comparisons showed R1 and T1 conditions were clearly discriminated, highlighting that these may be used as host biomarkers to PM response. At the same time, in panel D data of T0 DETs (Panel D of Fig. 3) showed a specific cluster remark that these DETs can be

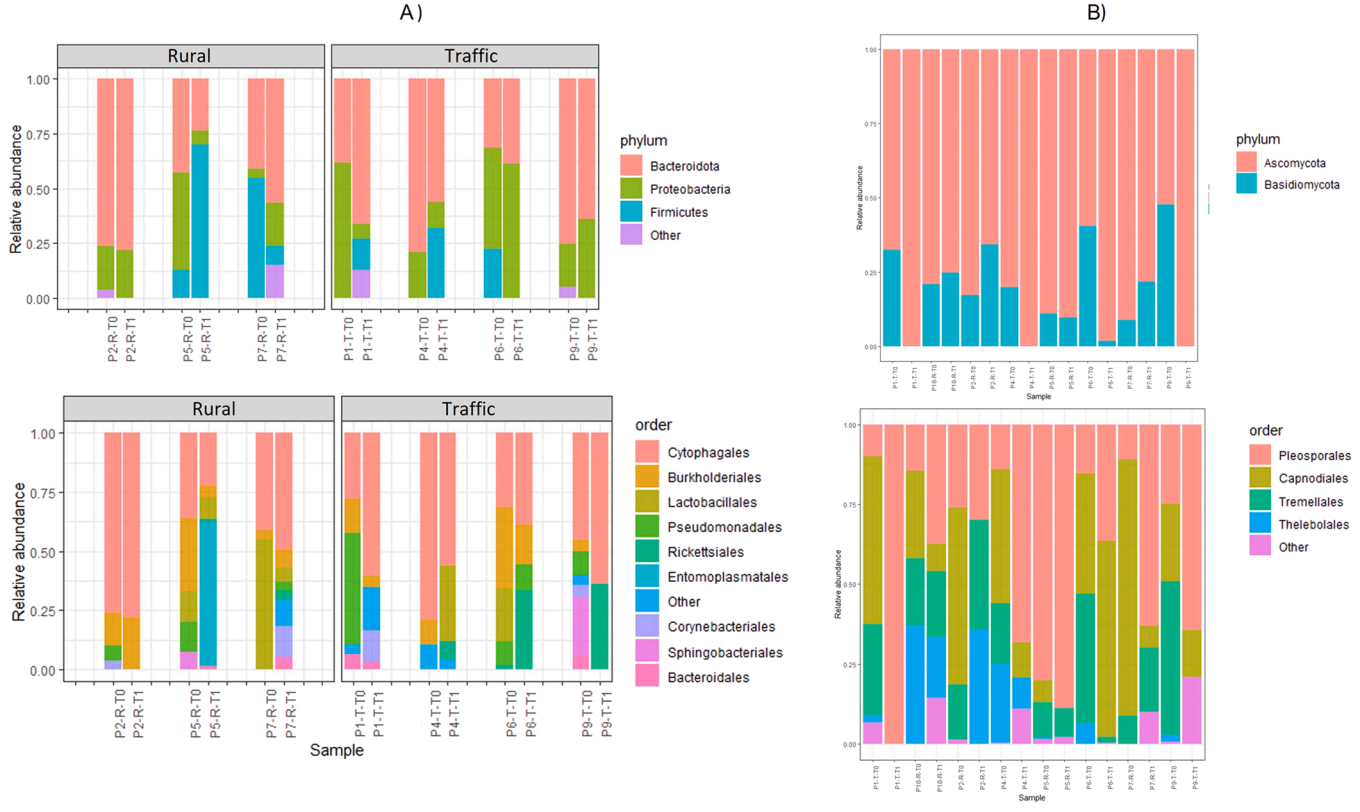

Fig. 9. Relative abundances of taxonomies at the phylum and order levels, in relation to sampling area. A) Bacteria; B) Fungi.

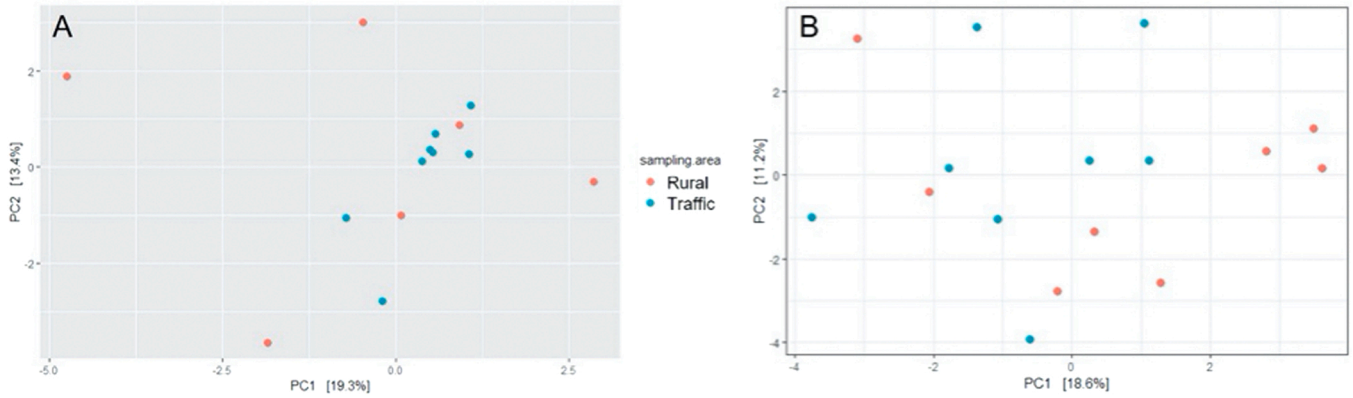

Fig. 10. PCA applied to the centered log-ratio (CLR) transformed counts Colours indicate the sampling time. A) Bacteria; B) Fungi.

Table 3
Permutational Multivariate Analysis of Variance (PERMANOVA) after a centered log ratio (CLR) transformation of microbiota for sampling date and area. The degree of freedom (Df), sum of squares, R2 F values and p values are reported.

A) Bacterial community

	Df	SumOfSqs	R2	F	Pr(>F)
Sampling area	1	45258	0.09851	1.3702	0.08659
Sampling date	1	37826	0.08234	1.1452	0.16078
Sampling area: sampling date	1	46029	0.10019	1.3936	0.07899
Residual	10	330290	0.71895		
Total	13	459404	1		

B) Fungal community

	Df	SumOfSqr	R2	F	Pr(>F)
samping area	1	484356	0.12296	2.542	0.05349
sampling date	1	707157	0.17952	3.711	0.00330 * *
sampling area:sampling date	1	460956	0.11702	2.419	0.06589
Residual	12	2286720	0.58051		
Total	15	3939189	1		

Table 4
Differential abundances of microbial ASVs in relation to sampling site and date. Results from DeSeq2 analysis are reported. The log2 fold change (Log2Fc), the p-value of contrast and the genus assigned to the ASV are indicated. The complete list of values obtained is reported in the Supplemental Dataset S1.

A)Bacterial community

Site	Contrast	ASV	Log2Fc	P-value	Genus
rural area	T1 vs T0	ASV11	20,825130	8.5843e-06	*Spiroplasma*

B) Fungal community

Site	Contrast	ASV	Log2Fc	P-value	Genus
rural area	T1 vs T0	ASV1	11.2748052	0.002	*Epicoccum*
traffic	T1 vs T0	ASV3	-10.291588	0.01	*Dioszegia*

considered specific biomarkers of leaf development.

4.1. PM effects on the leaf primary metabolism

It is known that the toxic effects of PM on plants deals with a decrease of leaf dry matter, increased concentrations of trace elements and nitrates in the above-ground biomass, changes in leaf gas-exchange parameters and amino acid concentrations (Cape et al., 2009). It has been suggested that the shading effects due to deposition of suspended PM on the leaf surface might be responsible for the decrease in the concentration of chlorophyll in polluted area (Popek et al., 2018). The reduction in chlorophyll content is expected to affect photosynthesis (Chauhan, 2010; Pandey et al., 2017). However, our transcriptomic data did not show any clear reduction of photosynthesis-related genes in T compared to R. Other studies dealing with dust particulate matter (iron) stress have shown an impairment of glycolysis and TCA pathways (Kuki et al., 2008). In addition, particulate matter levels showed to affect the activity of several enzymes involved in photorespiration such as glycolate oxidase and phosphoenol pyruvate carboxylase (Mandal, 2006). Interestingly, our data partially agreed with these previous findings. TCA and mitochondrial electron transport pathways were induced in R but not in T. In addition, we found that *phosphoglucomutase and sugar isomerase* (*SIS*) were upregulated in rural area but not in traffic area implying an inhibition effect of PM on gluconeogenesis.

We observed the repression of some genes involved in aminoacid biosynthesis by high levels of PM like *Asn1* (*Glutamine-dependent asparagine synthase 1*), *Pgdh* (*3-phosphoglycerate dehydrogenase*) and *Hog1* 2 (*High osmolarity glycerol*). This evidence was expected since we have examined a long-term response to chronic stress (three months). Indeed, plants are subjected to PM stress for a long time with a consequent chronic inhibitory effect of photosynthesis due to the reduced amount of natural light received by leaf tissues. A significant reduction of photosynthetic activity was also observed in a previous study dealing with similar periods of PM accumulation in mature leaves of different plant species (Cuba et al., 2020). PM has been shown to change the pools of free glutamate and asparagine metabolized during photorespiration (Vega, 2018). Glutamate, glutamine, aspartate and asparagine are used to transfer nitrogen from source organs to sink tissues and to build up reserves during periods of nitrogen availability for subsequent use in growth, defense and reproductive processes (Hernández-Jiménez et al., 2002; Ogawa and Iwabuchi, 2001). Our study seems to confirm these findings, since we observed some key genes involved in TCA, gluconeogenesis and photorespiration like *Sdh2–1* (*Succinate dehydrogenase* [ubiquinone] *iron-sulfur subunit 1*), *Sdh1–2* (*Succinate dehydrogenase* [ubiquinone] *flavoprotein subunit 2*), *Mls* (*malate synthase*), *Icl* (*isocitrate lyase*) *and Gdch* (*Glycine decarboxylase complex*) that were down-regulated by high level of PM. No studies have been conducted on particulate matter at the transcriptomic level. Previous studies have focused on other pollutants like SO_2, NO_2 and H_2S under hardening conditions which can cause more depletion of soluble sugars in the leaves of plants grown in polluted area. Other dust particulate matter (iron) has shown a reduced pH and consequently impairs of glycolysis process in two costal plant species (Kuki et al., 2008).

Relating to lipid metabolism, our results showed that the transcript abundance of two key genes, *Acyl-coenzyme a desaturase-like2* and *Delta 9 desaturase 1* were higher in R than in T. These genes are involved in the synthesis of chloroplast lipids and VLCFAs (very-long-chain fatty acids) of certain seed oils. These proteins have a role in petal senescence and are involved in temperatures changes (Byun et al., 2014). Another member of these gene family, has been suggested to have a potential role

in drought tolerance (Wisutiamonkul et al., 2017). Previous evidence suggests that *Acyl-coenzyme a desaturase-like2* play a significant role in determining the degree of unsaturation of membrane lipids, and particularly in sphingolipids which have a key role in response to low temperature (Esmaeili et al., 2021). We hypothesize that these genes might be involved in modulating the leaf cell membrane fluidity which may be a key factor in sensing PMs deposition in leaves. Dust caused by air pollution showed to damage leaf physiological functions in cotton leaves, reducing leaf chlorophyll and carotenoid content and increasing cytoplasmic membrane permeability, leaf cellular structure, leaf blade surface morphology(Abuduwaili et al., 2015).

4.2. Stress response pathways

4.2.1. Biotic stress responses

We observed an increased expression of biotic stress-related genes in T compared to R. This phenomenon is well-known and occurred in previous meta-analysis of transcriptomic responses to abiotic stresses. In response to drought plants activated transcription factors involved in biotic response were induced (WRKY20, Alfin-like 1, Set26) and several GO-terms such as response to nematode, ethylene-signaling) (Benny et al., 2019). In addition, different abiotic stresses (drought, salinity) showed the induction of genes involved in biotic stress responses (terpenoid, phenol, and anthocyanin biosynthesis) as well as specific biotic stress-related genes such as *TINY*, *CCR* (*cinnamoil CoA reductases*), several members of *WRKYs* involved in crosstalk between biotic and abiotic stress (Balti et al., 2021). In addition, cold stress induced several genes involved in response to pathogen infections such as *lipoxygenases*, *NAC transcription factors*, *pathogenesis-related thaumatin proteins*, *disease resistance proteins* (*CC-NBS-LRR*) (Vergata et al., 2022). On the other hand, several abiotic stress-related genes were also induced in response to different categories of pathogen (Balan et al., 2017). Genes such as *Atlp-1(Putative pathogenesis-related thaumatin superfamily protein), Atprb1 (Putative basic pathogenesis-related protein 1)* and *Q19e69 (Disease resistance protein)* were upregulated in the plants grown in traffic conditions. The same categories of genes were also induced by cold stress (Vergata et al., 2022). *Atlp-1* and *Atprb1* were member of TLP family that have essential functions in plant development and response to adversity stresses (Singh et al., 2013). Thaumatin like proteins (TLPs) are vital proteins involved in the complex defense process of plant pathogens. Members of the TLP family have been reported in recent studies to participate in multiple biological processes under biotic or abiotic stress (Petre et al., 2011). Recently, it has been shown that *GbTLPs* in *Gossypium barbadense* were significantly upregulated after *Verticillium dahliae* infection, suggesting a role for TLP in disease resistance (Zhang et al., 2021). Furthermore, the tolerance of tobacco to salt, oxidative, and drought stress was enhanced by *AdTLPs* expression (Barthakur et al., 2001; Singh et al., 2013). In addition to antibiotic activities, *TLPs* have also been involved in other physiological and developmental roles, including antifreeze activities (Yu and Griffith, 1999), abiotic stress tolerance (Subramanyam et al., 2012), floral organ formation and fruit ripening (Neale et al., 1990) and glucanase activity (Osmond et al., 2001). *Ctl2* is a member of class II chitinase and evidences in *Arabidopsis* and poplar suggest that CTL proteins play important roles in primary and secondary cell wall formation (Grover, 2012). This gene has been shown to be strongly upregulated in concert with secondary cell formation during interfascicular fibers differentiation in *Arabidopsis*. In poplar and *Arabidopsis*, expression of a specific chitinase member gene is highly correlated with secondary wall formation (Johnston, 2006). We found that Pathogenesis-related proteins were more induced in T conditions. The abundance of these proteins in tobacco leaves infected with various pathogens indicated that these proteins are involved in plant systemic responses to disease. Overexpression of the *PR-1* gene results in increased plant resistance to fungi, oomycetes, and bacteria, but not to viruses (Shin et al., 2014). *DIR6* (*disease resistance-responsive family protein*), member of the *DIR* family genes, plays a role in specific tissues at certain stages of plant growth and development. Previous reports have shown that the *DIR* genes were involved in abiotic stress. *BhDIR1* of *B. hygrometrica* responded to various abiotic stresses, including drought, $CaCl_2$, ABA, H_2O_2, and EGTA (Wu et al., 2009). *T. androssowii Tadir* gene was upregulated under salt and saline stress (Gao et al., 2010). *Saccharum* spp. *ScDir* expression was increased when seedlings were exposed to hydrogen peroxide, PEG and salt stress (Jin-Long et al., 2012).

In conclusion, we may provide the following explanation for the upregulation of biotic stress-related genes:

1) Many of the genes involved in defense pathways against environmental conditions are in common between abiotic and biotic stresses. The signalling cascades of these two main categories are overlapping and many genes are involved in crosstalk of the complex regulatory responses to biotic and abiotic stresses. In addition, several genes have common function of reducing reactive oxygen species, inactivate other toxic compounds, anti-oxidant properties.
2) It is also possible that particulate matter is also vehicle of pathogen infections and an increase of attacks may occur in leaves subjected to higher levels of PMs
3) PMs may render plants more sensitive to biotic stresses and this induce the expression of defense genes in response to a possible increase of pathogenic attacks (linked to the above explanation).

4.2.2. Abiotic stress responses

In this work, we observed an induction of several genes encoding key enzymes involved in redox pathways such as *protein disulfide isomerase* (thioredoxin family), *cytochrome B5 isoform C* and *ascorbate peroxidase 2* and *5* (ascorbate/glutathione), *Fe-superoxide dismutase 1* and *2* (dismutase/catalase). Although more genes involved in redox were induced in R than in T, most of them were in common. We may speculate that this occurs because in R the levels of PMs are anyway high enough to induce a defense response in plants while in T the levels are too high to allow an activating response of plants that are probably close to senescence stage. Indeed, it is well-accepted that abiotic stress typically leads to the overproduction of reactive oxygen species (ROS) in plants, which are highly reactive and toxic and cause damage to biological molecules. Non-enzymatic low molecular weight metabolites, such as ascorbate, glutathione and α-tocopherol help counteracting this process. These antioxidants are also capable of chelating metal ions, reducing thus their catalytic activity to form ROS and also scavenge them. Hence, in plant cells, this triad of low molecular weight antioxidants (ascorbate, glutathione and α-tocopherol) form an important part of abiotic stress response.

These pollutants affect plant growth either by displacement of essential cations from specific binding sites or generation of oxidative stress by the generation of ROS. One direct way of disruption was, upon uptake into the cell, a direct reaction took place with proteins due to an affinity for Thionyl-, Histidyl- and Carboxyl- groups (Kumar et al., 2017; Sharma and Dietz, 2009).

In the literature, although no studies are reported on PMs, many studies have shown that HSPs were induced in response to various abiotic stresses including heavy metals (ÇELİK et al., 2021). Similarly, the *HSP70* sub-family, DnaK (Bip), was up-regulated in rice seedlings (Rodríguez-Celma et al., 2010). *Arabidopsis* exposure to cadmium stress induced many *HSPs* (Lee and Ahn, 2013). Similarly, increased expression was reported for *HSP80* and *HSP17.9* in rice (Ahsan et al., 2007). We observed that a member of the class I small heat-shock protein (*sHSP*) family, was upregulated only in T conditions in our experiment, according to the same trend previously studied and described in the literature.

On the other hand, HSP*70–13*, a member of the HSP70 family of heat shock proteins was downregulated in T conditions. Hossain et al. (2013), described that in soybeans, two-folds higher accumulation of *HSP* was recorded in Cd-accumulating genotypes, while there was less *HSP70*

expression in lower Cd-accumulating varieties, which showed that *HSP* expression was also genotype-specific (Hossain et al., 2012). Proteins of the RmlC-like family in rice are involved in antioxidant defense and detoxification during Cu-induced oxidative stress (Chen et al., 2015). To overcome oxidative stress, plants often recruit enzymatic components such as superoxide dismutase (SOD), catalase (CAT), peroxidase (POD), and so forth. Protective responses against abiotic stress often go through the formation of active oxygen forms, and therefore, the ROC3 interaction with *At5g39120* can regulate ROS accumulation in plant tissues to generate defensive response. *RmlC-like cupins superfamily protein* was upregulated in T highlighting that this gene may be involved in PM response. We also observed the PM modulation of some genes encoding proteins involved in detoxification of oxygen radicals.

Heavy metals induce the synthesis of organic ligands that could form metal complexes with reduced biological activity. When plants are exposed to heavy metals, PCS (phytochelatin synthase, an enzyme that synthesized phytochelatins (PC) from glutathione (GSH) and homologous biothiols) condenses the γ-glutamyl-cysteine moiety of a GSH molecule with the glutamic acid residue of a second GSH, releasing glycine and increasing the length of the PC molecule. *Arabidopsis* plants treated with cadmium or copper responded by increasing transcription of the genes for glutathione synthesis and reduction, γ-ECS and GSH-S, as well as GR.

4.3. Cell cycle and cell division

Trivedi et al. (2012) in their study in *Arabidopsis*, indicated that *cyclophilin family* genes were less responsive to various stresses as compared with the rice cyclophilins. A cyclophilin with peptidyl-prolyl *cis-trans* isomerase activity (*CYP2*) was upregulated in T. Since cyclophilins have been associated with a wide range of processes (including signal transduction), they have been found to catalyze the folding of certain proteins while serving as molecular chaperones (Godoy et al., 2000).

Genes involved in cell cycle in our experimental condition were upregulated in R compared to T implying that the oxidative stress in traffic conditions might be correlated with a decrease in cell cycle processes compared to rural conditions. In plants, very few data are available on the possible link between abiotic stress responses and cell cycle progression. Logemann et al. (1995) showed a tight correlation between down-regulation of cell cycle genes and up-regulation of defense genes following UV irradiation or elicitor treatment in parsley cells. This study examined the impact of oxidative stress on the cell cycle progression using the redox-cycling drug menadione. Reichheld et al. (1999) demonstrated that mild oxidative stress leads to inhibition of cell division both in cell suspension and plants. Mild oxidative stress during the S phase slows down progression into the S phase and delays entry into mitosis, transiently blocking cells in G2. and underline the existence of specific mechanisms responsible for transient cell cycle blocking at different checkpoints in response to sublethal menadione-induced oxidative stress.

4.4. Transcription factors involved in PM response

Our transcriptomic analysis highlighted that some key transcription factors like *G2-like, C3H* and *Myb* were involved in response to PM stress. The relation between different expression of transcription factors and plants exposed to different concentrations of heavy metals is well-known. Gao et al. (2015) described transcriptomic changes during maize root development responsive to Pb highlighting the role on Pb responses of *C2H2* zinc finger family bHLH (*bZIP*), *AP2/EREBP, APETALA2*/Ethylene-responsive element binding protein family (*ERF*) as well as G*2-like transcription factor family (GARP*). At the same time, Sapara et al. (2019),identified several MYB members in response to heavy metal stress. *Myb* transcription factor plays important role in stress tolerance by ABA-dependent and -independent mode. The rice *Myb* TFs were upregulated on exposure to cadmium stress at different time durations (Ogawa et al., 2009). Similarly, in *Arabidopsis* also different *Mybs* (*Myb4*, *Myb28*, *Myb43*, *Myb48*, *Myb72* and *Myb124*) were induced by Cd and Zn metal stress, and mutant *Myb72* exhibits metal sensitivity (Van De Mortel et al., 2008).

4.5. Microbiota

The leaf associated microbiota was not significantly different between the rural and the traffic area for what concerns bacteria, allowing to conclude that the bacterial community populating *Photinia* leaves is resilient to PM exposure, partially in line with previous observations concerning other environmental perturbations (Almario et al., 2022; Chaudhry et al., 2021). This evidence was expected since the two different areas were highly close each other (<2 km) within the same Municipality and main environmental parameters were similar. Bacterial community is affected by many other environmental factors (temperature, water and nutrient availability, light intensity, plant developmental stage, soil conditions) causing a significant level of uncontrolled variability that probably render differences not significant. However, an interesting exception was found for a microbial genus, *Spiroplasma* sp., and two fungal genera, *Epicoccum* sp. and *Dioszegia* sp., which are known to be associated with plants (Regassa and Gasparich, 2006; Taguiam et al., 2021; Zhang and Yao, 2015). *Spiroplasma* sp. is known to be mainly transmitted to plants by insect vectors (Regassa and Gasparich, 2006). Since in urban areas insect communities are less abundant and less rich in species (Theodorou, 2022), we may hypothesize that plants in rural era were more susceptible to this interaction. The differences of *Epicoccum* sp. in rural area samples, where PM accumulation was lower, lead to hypothesize that this genus is more susceptible to PM exposure and to the physiological conditions of the plants related to high PM exposure. *Epicoccum* spp. are endophytic ascomycetes that include both species able to cause plant diseases, and species with biological control activity against plant pathogens (Taguiam et al., 2021). Therefore, we may hypothesize that, given the health status of the plants, this shift was beneficial for *Photinia* plants. In contrast, *Dioszegia* sp. was more associated with differences during exposure to the traffic zone, suggesting its decrease as indicator of PM exposure. Members of the genus *Dioszegia* (Basidiomycota) are known as epiphytic yeasts of the phyllosphere (Wang et al., 2016; Zhang and Yao, 2015). Interestingly, *Dioszegia* sp. has been reported to occupy a central position in the plant microbial network and, as such, to shape the leaf microbiota in response to host or abiotic factors (Agler et al., 2016). For this reason, it is tempting to speculate that the *Dioszegia* species may act as sentinel microbe for the effect PM accumulation may have on the leaf-associated microbiota. Moreover, it would be interesting to investigate the mutual interaction between such differences in *Dioszegia* and *Epicoccum* and the plant transcriptome. In fact, modulation of gibberellin signalling is observed upon fungal colonization (Buhrow et al., 2021), as well as flavonoid biosynthesis, which play important role in pathogenic fungal defence (Förster et al., 2021). We may tentatively hypothesize that part of the differences in the plant transcriptome observed here may affect, or be affected by, the leaf-associated microbiota and in particular its fungal fraction. However, experiments in controlled conditions are needed to test such a hypothesis by artificially modifying the leaf microbiota.

5. Conclusions

A summarized picture of the main transcriptomic changes to PMs responses has been provided in Fig. 11. The most repressed pathways by PMs accumulation belonged to primary metabolism such as glycolysis, gluconeogenesis and TCA cycle. These inhibitory effects on pathways involved in carbon assimilation should drive a repression on defence response pathway through the modulation of the physiological response to PMs stress and the induction of three TF families (G2-like, C3H,

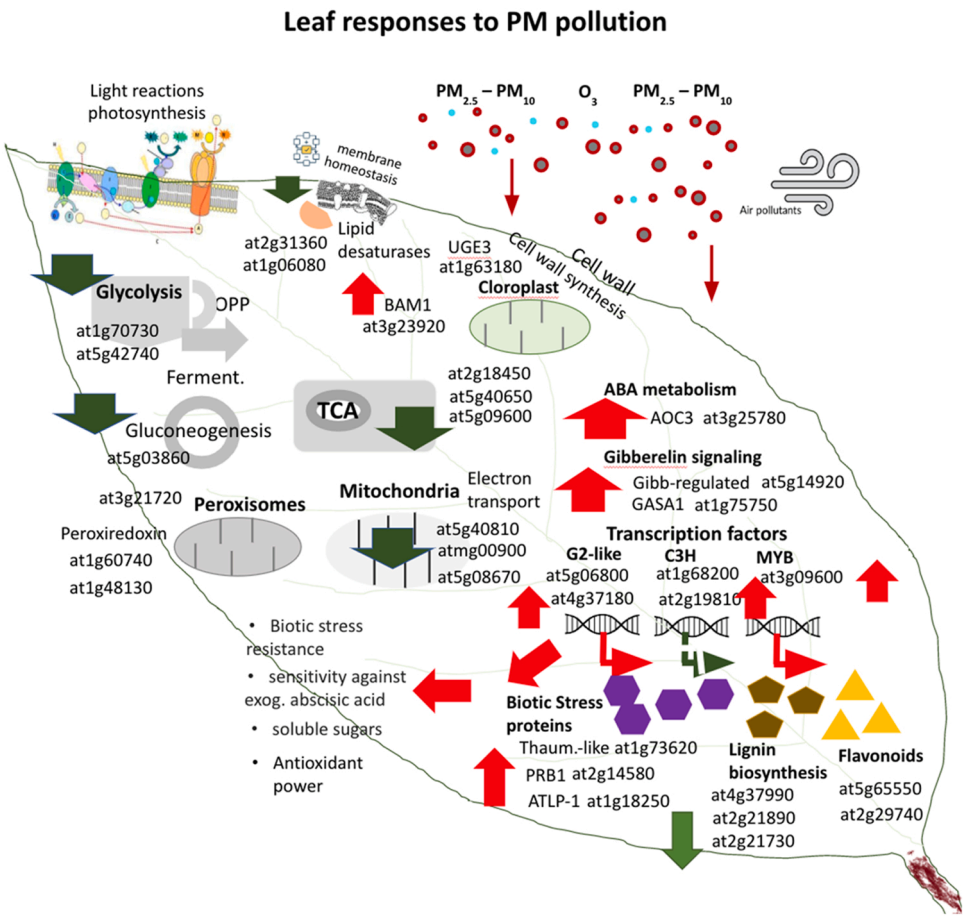

Fig. 11. Summary of the main gene regulatory networks in response to PM pollution. Green arrows mean downregulated while red ones mean upregulated.

MYBs). Several genes involved in biotic stress (thaumatin like proteins), lignin biosynthesis and secondary metabolism were induced in traffic conditions. This work should enhance other future studies dealing with the identification of genes involved in PMs stress tolerance to develop biotechnological approaches for phylloremediation of PMs, highly dangerous for human health and environment in general.

Funding

This research has been funded by Fondazione Cassa di Risparmio di Lucca (project Acronym: VEG-LU-PM10).

CRediT authorship contribution statement

Conceptualization: Federico Martinelli. Software: Felice Contaldi, Matteo Buti. Validation: Chiara Vergata, Felice Contaldi. Investigation: Federico Martinelli, Chiara Vergata, Felice Contaldi, Ivan Baccelli, Francesco Pecori, Alberto Santini, Alessio Mengoni, Francesca Vaccaro, Francesco Ferrini, Barbara Basso Moura. Writing - Original Draft: Chiara Vergata, Felice Contaldi, Federico Martinelli. Writing - Review & Editing: all authors. Funding acquisition: Federico Martinelli.

Declaration of Competing Interest

The authors declare that they have no known competing financial interests or personal relationships that could have appeared to influence the work reported in this paper.

Data Availability

The data that has been used is confidential.

Appendix A. Supporting information

Supplementary data associated with this article can be found in the online version at doi:10.1016/j.envexpbot.2023.105313.

References

Abhijith, K., Kumar, P., Gallagher, J., McNabola, A., Baldauf, R., Pilla, F., Broderick, B., Di Sabatino, S., Pulvirenti, B., 2017. Air pollution abatement performances of green infrastructure in open road and built-up street canyon environments–a review. Atmos. Environ. 162, 71–86.

Abuduwaili, J., Zhaoyong, Z., Feng qing, J., Dong wei, L., 2015. The disastrous effects of salt dust deposition on cotton leaf photosynthesis and the cell physiological properties in the Ebinur Basin in Northwest China. PLOS ONE 10, e0124546.

Afgan, E., Baker, D., Batut, B., van den Beek, M., Bouvier, D., Cech, M., Chilton, J., Clements, D., Coraor, N., Gruning, B.A., Guerler, A., Hillman-Jackson, J., Hiltemann, S., Jalili, V., Rasche, H., Soranzo, N., Goecks, J., Taylor, J., Nekrutenko, A., Blankenberg, D., 2018. The galaxy platform for accessible, reproducible and collaborative biomedical analyses: 2018 update. Nucleic Acids Res 46, W537–W544.

Agler, M.T., Ruhe, J., Kroll, S., Morhenn, C., Kim, S.-T., Weigel, D., Kemen, E.M., 2016. Microbial hub taxa link host and abiotic factors to plant microbiome variation. PLOS Biol. 14, e1002352.

Ahsan, N., Lee, S.-H., Lee, D.-G., Lee, H., Lee, S.W., Bahk, J.D., Lee, B.-H., 2007. Physiological and protein profiles alternation of germinating rice seedlings exposed to acute cadmium toxicity. Comptes rendus Biol. 330, 735–746.

Almario, J., Mahmoudi, M., Kroll, S., Agler, M., Placzek, A., Mari, A., Kemen, E., 2022. The leaf microbiome of arabidopsis displays reproducible dynamics and patterns throughout the growing season. mBio 13, e0282521.

Andrews, S., 2010. FastQC: a quality control tool for high throughput sequence data. Babraham Bioinformatics, Babraham Institute, Cambridge, United Kingdom.

Balan, A.K., Mottakkunnu Parambil, S., Vakyath, S., Thulissery Velayudhan, J., Naduparambath, S., Etathil, P., 2017. Coconut shell powder reinforced thermoplastic polyurethane/natural rubber blend-composites: effect of silane coupling agents on the mechanical and thermal properties of the composites. J. Mater. Sci. 52, 6712–6725.
Balti, I., Benny, J., Perrone, A., Caruso, T., Abdallah, D., Salhi-Hannachi, A., Martinelli, F., 2021. Identification of conserved genes linked to responses to abiotic stresses in leaves among different plant species. Funct. Plant Biol. 48, 54–71.
Barthakur, S., Babu, V., Bansa, K.C., 2001. Over-expression of osmotin induces proline accumulation and confers tolerance to osmotic stress in transgenic tobacco. J. Plant Biochem. Biotechnol. 10, 31–37.
Benny, J., Pisciotta, A., Caruso, T., Martinelli, F., 2019. Identification of key genes and its chromosome regions linked to drought responses in leaves across different crops through meta-analysis of RNA-Seq data. BMC Plant Biol. 19, 194.
Bolger, A.M., Lohse, M., Usadel, B., 2014. Trimmomatic: a flexible trimmer for Illumina sequence data. Bioinformatics 30, 2114–2120.
Buhrow, L.M., Liu, Z., Cram, D., Sharma, T., Foroud, N.A., Pan, Y., Loewen, M.C., 2021. Wheat transcriptome profiling reveals abscisic and gibberellic acid treatments regulate early-stage phytohormone defense signaling, cell wall fortification, and metabolic switches following Fusarium graminearum-challenge. BMC Genom. 22, 798.
Byun, Y.J., Koo, M.Y., Joo, H.J., Ha-Lee, Y.M., Lee, D.H., 2014. Comparative analysis of gene expression under cold acclimation, deacclimation and reacclimation in Arabidopsis. Physiol. Plant. 152, 256–274.
Callahan, B.J., McMurdie, P.J., Rosen, M.J., Han, A.W., Johnson, A.J., Holmes, S.P., 2016. DADA2: high-resolution sample inference from Illumina amplicon data. Nat. Methods 13, 581–583.
Camacho, C., Coulouris, G., Avagyan, V., Ma, N., Papadopoulos, J., Bealer, K., Madden, T.L., 2009. BLAST+: architecture and applications. BMC Bioinforma. 10, 421.
Cangioli, L., Mancini, M., Baldi, A., Fagorzi, C., Orlandini, S., Vaccaro, F., Mengoni, A., 2022. Effect of site and phenological status on the potato bacterial rhizomicrobiota. Microorganisms 10.
Cape, J.N., Hamilton, R., Heal, M.R., 2009. Reactive uptake of ozone at simulated leaf surfaces: Implications for 'non-stomatal' ozone flux. Atmos. Environ. 43, 1116–1123.
ÇELİK, E.N.Y.B., MEHMET CENGİZ, SEZGİN, A.Y.A.N., 2021. Gene expression profiles of Hsp family members in different poplar taxa under cadmium stress. Turk. J. Agric. For. 45.
Chaudhry, V., Runge, P., Sengupta, P., Doehlemann, G., Parker, J.E., Kemen, E., 2021. Shaping the leaf microbiota: plant-microbe-microbe interactions. J. Exp. Bot. 72, 36–56.
Chauhan, A., 2010. Effect Of Ambient Air Pollutants On Wheat and Mustard Crops Growing In The Vicinity Of Urban and Industrial Areas.
Chen, L., Liao, B., Qi, H., Xie, L.-J., Huang, L., Tan, W.-J., Zhai, N., Yuan, L.-B., Zhou, Y., Yu, L.-J., 2015. Autophagy contributes to regulation of the hypoxia response during submergence in Arabidopsis thaliana. Autophagy 11, 2233–2246.
Cheng, C.Y., Krishnakumar, V., Chan, A.P., Thibaud-Nissen, F., Schobel, S., Town, C.D., 2017. Araport11: a complete reannotation of the Arabidopsis thaliana reference genome. Plant J. 89, 789–804.
Dennis Jr., G., Sherman, B.T., Hosack, D.A., Yang, J., Gao, W., Lane, H.C., Lempicki, R.A., 2003. Genome Biol, 4. Database for Annotation, Visualization, and Integrated Discovery, DAVID, p. P3.
Dirlewanger, E., Graziano, E., Joobeur, T., Garriga-Calderé, F., Cosson, P., Howad, W., Arús, P., 2004. Comparative mapping and marker-assisted selection in Rosaceae fruit crops. Proc. Natl. Acad. Sci. 101, 9891–9896.
Doyle, J.J., Doyle, J.L., 1987. A rapid DNA isolation procedure for small quantities of fresh leaf tissue.
Dzierżanowski, K., Popek, R., Gawrońska, H., Sæbø, A., Gawroński, S.W., 2011. Deposition of particulate matter of different size fractions on leaf surfaces and in waxes of urban forest species. Int. J. Phytoremediat. 13, 1037–1046.
Esmaeili, N., Cai, Y., Tang, F., Zhu, X., Smith, J., Mishra, N., Hequet, E., Ritchie, G., Jones, D., Shen, G., 2021. Towards doubling fibre yield for cotton in the semiarid agricultural area by increasing tolerance to drought, heat and salinity simultaneously. Plant Biotechnol. J. 19, 462–476.
Espenshade, J., Thijs, S., Gawronski, S., Bové, H., Weyens, N., Vangronsveld, J., 2019. Influence of urbanization on epiphytic bacterial communities of the platanus × hispanica tree leaves in a biennial study. Front. Microbiol. 10.
Fang, T., Jiang, T., Yang, K., Li, J., Liang, Y., Zhao, X., Gao, N., Li, H., Lu, W., Cui, K., 2021. Biomonitoring of heavy metal contamination with roadside trees from metropolitan area of Hefei, China. Environ. Monit. Assess. 193, 1–14.
Förster, C., Handrick, V., Ding, Y., Nakamura, Y., Paetz, C., Schneider, B., Castro-Falcón, G., Hughes, C.C., Luck, K., Poosapati, S., Kunert, G., Huffaker, A., Gershenzon, J., Schmelz, E.A., Köllner, T.G., 2021. Biosynthesis and antifungal activity of fungus-induced O-methylated flavonoids in maize. Plant Physiol. 188, 167–190.
Fu, L., Niu, B., Zhu, Z., Wu, S., Li, W., 2012. CD-HIT: accelerated for clustering the next-generation sequencing data. Bioinformatics 28, 3150–3152.
Gao, C., Liu, G., Wang, Y., Jiang, J., Yang, C., 2010. Cloning and analysis of dirigent-like protein in gene from Tamarix androssowii. Bull. Bot. Res. 30, 81–86.
Gao, J., Zhang, Y., Lu, C., Peng, H., Luo, M., Li, G., Shen, Y., Ding, H., Zhang, Z., Pan, G., Lin, H., 2015. The development dynamics of the maize root transcriptome responsive to heavy metal Pb pollution. Biochem. Biophys. Res. Commun. 458, 287–293.
Gawronski, S.W., Gawronska, H., Lomnicki, S., Sæbo, A., Vangronsveld, J., 2017. Chapter Eight - Plants in Air Phytoremediation. In: Cuypers, A., Vangronsveld, J. (Eds.), Advances in Botanical Research. Academic Press, pp. 319–346.
Godoy, A.V., Lazzaro, A.S., Casalongué, C.A., San Segundo, B., 2000. Expression of a Solanum tuberosum cyclophilin gene is regulated by fungal infection and abiotic stress conditions. Plant Sci. 152, 123–134.
Gourdji, S., 2018. Review of plants to mitigate particulate matter, ozone as well as nitrogen dioxide air pollutants and applicable recommendations for green roofs in Montreal, Quebec. Environ. Pollut. 241, 378–387.
Gouveia, N., Kephart, J.L., Dronova, I., McClure, L., Granados, J.T., Betancourt, R.M., O'Ryan, A.C., Texcalac-Sangrador, J.L., Martinez-Folgar, K., Rodriguez, D., Diez-Roux, A.V., 2021. Ambient fine particulate matter in Latin American cities: Levels, population exposure, and associated urban factors. Sci. Total Environ. 772, 145035.
Grabherr, M.G., Haas, B.J., Yassour, M., Levin, J.Z., Thompson, D.A., Amit, I., Adiconis, X., Fan, L., Raychowdhury, R., Zeng, Q., Chen, Z., Mauceli, E., Hacohen, N., Gnirke, A., Rhind, N., di Palma, F., Birren, B.W., Nusbaum, C., Lindblad-Toh, K., Friedman, N., Regev, A., 2011. Full-length transcriptome assembly from RNA-Seq data without a reference genome. Nat. Biotechnol. 29, 644–652.
Grover, A., 2012. Plant chitinases: genetic diversity and physiological roles. Crit. Rev. Plant Sci. 31, 57–73.
Guo, C., Lv, S., Liu, Y., Li, Y., 2022. Biomarkers for the adverse effects on respiratory system health associated with atmospheric particulate matter exposure. J. Hazard Mater. 421, 126760.
He, C., Qiu, K., Pott, R., 2020. Reduction of traffic-related particulate matter by roadside plants: effect of traffic pressure and sampling height. Int J. Phytoremediat. 22, 184–200.
Hernández-Jiménez, M.J., Lucas, M.M., de Felipe, M.R., 2002. Antioxidant defence and damage in senescing lupin nodules. Plant Physiol. Biochem. 40, 645–657.
Hirano, T., Kiyota, M., Aiga, I., 1995. Physical effects of dust on leaf physiology of cucumber and kidney bean plants. Environ. Pollut. 89, 255–261.
Hossain, Z., Hajika, M., Komatsu, S., 2012. Comparative proteome analysis of high and low cadmium accumulating soybeans under cadmium stress. Amino Acids 43, 2393–2416.
Hossain, Z., Khatoon, A., Komatsu, S., 2013. Soybean proteomics for unraveling abiotic stress response mechanism. J. Proteome Res. 12, 4670–4684.
Jin-Long, G., Li-Ping, X., Jing-Ping, F., Ya-Chun, S., Hua-Ying, F., You-Xiong, Q., Jing-Sheng, X., 2012. A novel dirigent protein gene with highly stem-specific expression from sugarcane, response to drought, salt and oxidative stresses. Plant Cell Rep. 31, 1801–1812.
Johnston, D.M., 2006. Functional genomics of plant chitinase-like genes.
Jouraeva, V.A., Johnson, D.L., Hassett, J.P., Nowak, D.J., 2002. Differences in accumulation of PAHs and metals on the leaves of Tilia× euchlora and Pyrus calleryana. Environ. Pollut. 120, 331–338.
Kandlikar, G.S., Gold, Z.J., Cowen, M.C., Meyer, R.S., Freise, A.C., Kraft, N.J.B., Moberg-Parker, J., Sprague, J., Kushner, D.J., Curd, E.E., 2018. ranacapa: An R package and Shiny web app to explore environmental DNA data with exploratory statistics and interactive visualizations. F1000Res 7, 1734.
Kończak, B., Cempa, M., Pierzchała, Ł., Deska, M., 2021. Assessment of the ability of roadside vegetation to remove particulate matter from the urban air. Environ. Pollut. 268, 115465.
Kovacs, K., West, G., Nowak, D.J., Haight, R.G., 2022. Tree cover and property values in the United States: a national meta-analysis. Ecol. Econ. 197, 107424.
Kuki, K.N., Oliva, M.A., Pereira, E.G., Costa, A.C., Cambraia, J., 2008. Effects of simulated deposition of acid mist and iron ore particulate matter on photosynthesis and the generation of oxidative stress in Schinus terebinthifolius Radii and Sophora tomentosa L. Sci. Total Environ. 403, 207–214.
Kumar, M., Padula, M.P., Davey, P., Pernice, M., Jiang, Z., Sablok, G., Contreras-Porcia, L., Ralph, P.J., 2017. Proteome analysis reveals extensive light stress-response reprogramming in the seagrass Zostera muelleri (Alismatales, Zosteraceae) metabolism. Front. Plant Sci. 7, 2023.
Larraburu, E.E., Apóstolo, N.M., Llorente, B.E., 2010. Anatomy and morphology of photinia (Photinia× fraseri Dress) in vitro plants inoculated with rhizobacteria. Trees 24, 635–642.
Lee, J., Ahn, Y.-J., 2013. Heterologous expression of a carrot small heat shock protein increased Escherichia coli viability under lead and arsenic stresses. HortScience 48, 1323–1326.
Leonard, R.J., McArthur, C., Hochuli, D.F., 2016. Particulate matter deposition on roadside plants and the importance of leaf trait combinations. Urban For. Urban Green. 20, 249–253.
Levy, A., Salas Gonzalez, I., Mittelviefhaus, M., Clingenpeel, S., Herrera Paredes, S., Miao, J., Wang, K., Devescovi, G., Stillman, K., Monteiro, F., Rangel Alvarez, B., Lundberg, D.S., Lu, T.-Y., Lebeis, S., Jin, Z., McDonald, M., Klein, A.P., Feltcher, M. E., Rio, T.G., Grant, S.R., Doty, S.L., Ley, R.E., Zhao, B., Venturi, V., Pelletier, D.A., Vorholt, J.A., Tringe, S.G., Woyke, T., Dangl, J.L., 2018. Genomic features of bacterial adaptation toplants. Nat. Genet. 50, 138–150.
Li, H., 2021. The complete chloroplast genome sequence of Photinia× fraseri, a medicinal plant and phylogenetic analysis. Mitochondrial DNA Part B 6, 2957–2959.
Li, J.W., Zhang, X.C., Wang, M.R., Bi, W.L., Faisal, M., da Silva, J.A.T., Volk, G.M., Wang, Q.C., 2019. Development, progress and future prospects in cryobiotechnology of Lilium spp. Plant Methods 15, 125.
Livak, K.J., Schmittgen, T.D., 2001. Analysis of relative gene expression data using real-time quantitative PCR and the 2(-Delta Delta C(T)) Method. Methods 25, 402–408.
Logemann, E., Parniske, M., Hahlbrock, K., 1995. Modes of expression and common structural features of the complete phenylalanine ammonia-lyase gene family in parsley. Proc. Natl. Acad. Sci. 92, 5905–5909.
Loomis, D., Grosse, Y., Lauby-Secretan, B., El Ghissassi, F., Bouvard, V., Benbrahim-Tallaa, L., Guha, N., Baan, R., Mattock, H., Straif, K., 2013. The carcinogenicity of outdoor air pollution. Lancet Oncol. 14, 1262.

Love, M.I., Huber, W., Anders, S., 2014. Moderated estimation of fold change and dispersion for RNA-seq data with DESeq2. Genome Biol. 15, 550.
Luo, X., Bing, H., Luo, Z., Wang, Y., Jin, L., 2019. Impacts of atmospheric particulate matter pollution on environmental biogeochemistry of trace metals in soil-plant system: A review. Environ. Pollut. 255, 113138.
Mandal, M., 2006. Physiological changes in certain test plants under automobile exhaust pollution. Foot 23 (17), 88.
McMurdie, P.J., Holmes, S., 2013. phyloseq: an R package for reproducible interactive analysis and graphics of microbiome census data. PLoS One 8, e61217.
Mori, J., Fini, A., Galimberti, M., Ginepro, M., Burchi, G., Massa, D., Ferrini, F., 2018. Air pollution deposition on a roadside vegetation barrier in a Mediterranean environment: Combined effect of evergreen shrub species and planting density. Sci. Total Environ. 643, 725–737.
Muhammad, S., Wuyts, K., Samson, R., 2020. Immobilized atmospheric particulate matter on leaves of 96 urban plant species. Environ. Sci. Pollut. Res. 27, 36920–36938.
Neale, A.D., Wahleithner, J.A., Lund, M., Bonnett, H.T., Kelly, A., Meeks-Wagner, D.R., Peacock, W.J., Dennis, E.S., 1990. Chitinase, beta-1, 3-glucanase, osmotin, and extensin are expressed in tobacco explants during flower formation. Plant Cell 2, 673–684.
Nilsson, R.H., Larsson, K.-H., Taylor, A.F.S., Bengtsson-Palme, J., Jeppesen, T.S., Schigel, D., Kennedy, P., Picard, K., Glöckner, F.O., Tedersoo, L., Saar, I., Kõljalg, U., Abarenkov, K., 2018. The UNITE database for molecular identification of fungi: handling dark taxa and parallel taxonomic classifications. Nucleic Acids Res. 47, D259–D264.
Ogawa, I., Nakanishi, H., Mori, S., Nishizawa, N.K., 2009. Time course analysis of gene regulation under cadmium stress in rice. Plant Soil 325, 97–108.
Ogawa, Ki, Iwabuchi, M., 2001. A mechanism for promoting the germination of Zinnia elegans seeds by hydrogen peroxide. Plant Cell Physiol. 42, 286–291.
Osmond, R.I., Hrmova, M., Fontaine, F., Imberty, A., Fincher, G.B., 2001. Binding interactions between barley thaumatin-like proteins and (1, 3)-β-D-glucans: Kinetics, specificity, structural analysis and biological implications. Eur. J. Biochem. 268, 4190–4199.
Pandey, G., Yadav, C.B., Sahu, P.P., Muthamilarasan, M., Prasad, M., 2017. Salinity induced differential methylation patterns in contrasting cultivars of foxtail millet (Setaria italica L.). Plant Cell Rep. 36, 759–772.
Park, J., Lim, C.J., Shen, M., Park, H.J., Cha, J.-Y., Iniesto, E., Rubio, V., Mengiste, T., Zhu, J.-K., Bressan, R.A., Lee, S.Y., Lee, B.-h, Jin, J.B., Pardo, J.M., Kim, W.-Y., Yun, D.-J., 2018. Epigenetic switch from repressive to permissive chromatin in response to cold stress. Proc. Natl. Acad. Sci. 115, E5400–E5409.
Perini, P., Pasquali, G., Margis-Pinheiro, M., de Oliviera, P.R.D., Revers, L.F., 2014. Reference genes for transcriptional analysis of flowering and fruit ripening stages in apple (Malus × domestica Borkh.). Mol. Breed. 34, 829–842.
Petre, B., Major, I., Rouhier, N., Duplessis, S., 2011. Genome-wide analysis of eukaryote thaumatin-like proteins (TLPs) with an emphasis on poplar. BMC Plant Biol. 11, 33.
Pikridas, M., Tasoglou, A., Florou, K., Pandis, S.N., 2013. Characterization of the origin of fine particulate matter in a medium size urban area in the Mediterranean. Atmos. Environ. 80, 264–274.
Popek, R., Przybysz, A., Gawronska, H., Klamkowski, K., Gawronski, S.W., 2018. Impact of particulate matter accumulation on the photosynthetic apparatus of roadside woody plants growing in the urban conditions. Ecotoxicol. Environ. Saf. 163, 56–62.
Popek, R., Mahawar, L., Shekhawat, G.S., Przybysz, A., 2022. Phyto-cleaning of particulate matter from polluted air by woody plant species in the near-desert city of Jodhpur (India) and the role of heme oxygenase in their response to PM stress conditions. Environ. Sci. Pollut. Res. 29, 70228–70241.
Prigioniero, A., Zuzolo, D., Niinemets, Ü., Postiglione, A., Mercurio, M., Izzo, F., Trifuoggi, M., Toscanesi, M., Scarano, P., Tartaglia, M., Sciarrillo, R., Guarino, C., 2022. Particulate matter and polycyclic aromatic hydrocarbon uptake in relation to leaf surface functional traits in Mediterranean evergreens: Potentials for air phytoremediation. J. Hazard. Mater. 435, 129029.
Pryor, J.T., Cowley, L.O., Simonds, S.E., 2022. The Physiological Effects of Air Pollution: Particulate Matter, Physiology and Disease. Front Public Health 10, 882569.
Quast, C., Pruesse, E., Yilmaz, P., Gerken, J., Schweer, T., Yarza, P., Peplies, J., Glockner, F.O., 2013. The SILVA ribosomal RNA gene database project: improved data processing and web-based tools. Nucleic Acids Res 41, D590–D596.
Rao, X., Huang, X., Zhou, Z., Lin, X., 2013. An improvement of the 2(-delta delta CT) method for quantitative real-time polymerase chain reaction data analysis. Biostat. Bioinforma. Biomath. 3, 71–85.
Redondo-Bermúdez, Md.C., Gulenc, I.T., Cameron, R.W., Inkson, B.J., 2021. 'Green barriers' for air pollutant capture: Leaf micromorphology as a mechanism to explain plants capacity to capture particulate matter. Environ. Pollut. 288, 117809.
Regassa, L.B., Gasparich, G.E., 2006. Spiroplasmas: evolutionary relationships and biodiversity. Front Biosci. 11, 2983–3002.
Reichheld, J.-P., Vernoux, T., Lardon, F., Van Montagu, M., Inzé, D., 1999. Specific checkpoints regulate plant cell cycle progression in response to oxidative stress. Plant J. 17, 647–656.
Robinson, M.D., McCarthy, D.J., Smyth, G.K., 2010. edgeR: a bioconductor package for differential expression analysis of digital gene expression data. Bioinformatics 26, 139–140.
Rodríguez-Celma, J., Rellán-Álvarez, R., Abadía, A., Abadía, J., López-Millán, A.-F., 2010. Changes induced by two levels of cadmium toxicity in the 2-DE protein profile of tomato roots. J. Proteom. 73, 1694–1706.
Sapara, K.K., Khedia, J., Agarwal, P., Gangapur, D.R., Agarwal, P.K., 2019. SbMYB15 transcription factor mitigates cadmium and nickel stress in transgenic tobacco by limiting uptake and modulating antioxidative defence system. Funct. Plant Biol. 46, 702–714.
Schraufnagel, D.E., Balmes, J.R., Cowl, C.T., De Matteis, S., Jung, S.H., Mortimer, K., Perez-Padilla, R., Rice, M.B., Riojas-Rodriguez, H., Sood, A., Thurston, G.D., To, T., Vanker, A., Wuebbles, D.J., 2019. Air pollution and noncommunicable diseases: a review by the forum of international respiratory societies' environmental committee, part 1: the damaging effects of air pollution. Chest 155, 409–416.
Shabnam, N., Oh, J., Park, S., Kim, H., 2021. Impact of particulate matter on primary leaves of Vigna radiata (L.) R. Wilczek. Ecotoxicol. Environ. Saf. 212, 111965.
Sharma, S.S., Dietz, K.-J., 2009. The relationship between metal toxicity and cellular redox imbalance. Trends Plant Sci. 14, 43–50.
Shin, S.H., Pak, J.-H., Kim, M.J., Kim, H.J., Oh, J.S., Choi, H.K., Jung, H.W., Chung, Y.S., 2014. An acidic pathogenesis-related1 gene of Oryza grandiglumis is involved in disease resistance response against bacterial infection. Plant Pathol. J. 30, 208.
Sillen, W.M.A., Thijs, S., Abbamondi, G.R., De La Torre Roche, R., Weyens, N., White, J. C., Vangronsveld, J., 2020. Nanoparticle treatment of maize analyzed through the metatranscriptome: compromised nitrogen cycling, possible phytopathogen selection, and plant hormesis. Microbiome 8, 127.
Simao, F.A., Waterhouse, R.M., Ioannidis, P., Kriventseva, E.V., Zdobnov, E.M., 2015. BUSCO: assessing genome assembly and annotation completeness with single-copy orthologs. Bioinformatics 31, 3210–3212.
Singh, N.K., Kumar, K.R., Kumar, D., Shukla, P., Kirti, P.B., 2013. Characterization of a pathogen induced thaumatin-like protein gene AdTLP from Arachis diogoi, a wild peanut. PLoS One 8, e83963.
Stacklies, W., Redestig, H., Scholz, M., Walther, D., Selbig, J., 2007. pcaMethods–a bioconductor package providing PCA methods for incomplete data. Bioinformatics 23, 1164–1167.
Subramanyam, K., Arun, M., Mariashibu, T.S., Theboral, J., Rajesh, M., Singh, N.K., Manickavasagam, M., Ganapathi, A., 2012. Overexpression of tobacco osmotin (Tbosm) in soybean conferred resistance to salinity stress and fungal infections. Planta 236, 1909–1925.
Syranidou, E., Thijs, S., Avramidou, M., Weyens, N., Venieri, D., Pintelon, I., Vangronsveld, J., Kalogerakis, N., 2018. Responses of the endophytic bacterial communities of juncus acutus to pollution with metals, emerging organic pollutants and to bioaugmentation with indigenous strains. Front. Plant Sci. 9.
Szklarczyk, D., Gable, A.L., Lyon, D., Junge, A., Wyder, S., Huerta-Cepas, J., Simonovic, M., Doncheva, N.T., Morris, J.H., Bork, P., Jensen, L.J., Mering, Christian v, 2018. STRING v11: protein–protein association networks with increased coverage, supporting functional discovery in genome-wide experimental datasets. Nucleic Acids Res. 47, D607–D613.
Taguiam, J.D., Evallo, E., Balendres, M.A., 2021. Epicoccum species: ubiquitous plant pathogens and effective biological control agents. Eur. J. Plant Pathol. 159, 713–725.
Theodorou, P., 2022. The effects of urbanisation on ecological interactions. Curr. Opin. Insect Sci. 52, 100922.
Thimm, O., Bläsing, O., Gibon, Y., Nagel, A., Meyer, S., Krüger, P., Selbig, J., Müller, L.A., Rhee, S.Y., Stitt, M., 2004. MAPMAN: a user-driven tool to display genomics data sets onto diagrams of metabolic pathways and other biological processes. Plant J. 37, 914–939.
Trivedi, D.K., Yadav, S., Vaid, N., Tuteja, N., 2012. Genome wide analysis of Cyclophilin gene family from rice and Arabidopsis and its comparison with yeast. Plant Signal. Behav. 7, 1653–1666.
Van De Mortel, J.E., Schat, H., Moerland, P.D., Ver Loren van Themaat, E., ENT, V.A.N.D. E.R., van der Ent, S., Blankestijn, H., Ghandilyan, A., Tsiatsiani, S., Aarts, MG., 2008. Expression differences for genes involved in lignin, glutathione and sulphate metabolism in response to cadmium in Arabidopsis thaliana and the related Zn/Cd-hyperaccumulator Thlaspi caerulescens. Plant. Cell. Environ. 31 (3), 301–324.
Vega, J.M., 2018. Nitrogen and sulfur metabolism in microalgae and plants: 50 years of research. Prog. Bot. Vol. 81, 1–40.
Vergata, C., Yousefi, S., Buti, M., Vestrucci, F., Gholami, M., Sarikhani, H., Salami, S.A., Martinelli, F., 2022. Meta-analysis of transcriptomic responses to cold stress in plants. Funct. Plant Biol. 49, 704–724.
Villanueva, R.A.M., Chen, Z.J., 2019. ggplot2: Elegant Graphics for Data Analysis. Taylor & Francis.
Wang, K., Sipilä, T.P., Overmyer, K., 2016. The isolation and characterization of resident yeasts from the phylloplane of Arabidopsis thaliana. Sci. Rep. 6, 39403.
Wei, X., Lyu, S., Yu, Y., Wang, Z., Liu, H., Pan, D., Chen, J., 2017. Phylloremediation of air pollutants: exploiting the potential of plant leaves and leaf-associated microbes. Front. Plant Sci. 8, 1318.
Wisutiamonkul, A., Ampomah-Dwamena, C., Allan, A.C., Ketsa, S., 2017. Carotenoid accumulation in durian (Durio zibethinus) fruit is affected by ethylene via modulation of carotenoid pathway gene expression. Plant Physiol. Biochem. 115, 308–319.
Wright, E.S., Yilmaz, L.S., Noguera, D.R., 2012. DECIPHER, a search-based approach to chimera identification for 16S rRNA sequences. Appl. Environ. Microbiol 78, 717–725.
Wu, R., Wang, L., Wang, Z., Shang, H., Liu, X., Zhu, Y., Qi, D., Deng, X., 2009. Cloning and expression analysis of a dirigent protein gene from the resurrection plant Boea hygrometrica. Prog. Nat. Sci. 19, 347–352.
Yu, H., Zhou, L., Dai, L., Shen, W., Dai, W., Zheng, J., Ma, Y., Chen, M., 2016. Nucleation and growth of sub-3 nm particles in the polluted urban atmosphere of a megacity in China. Atmos. Chem. Phys. 16, 2641–2657.
Yu, X.M., Griffith, M., 1999. Antifreeze proteins in winter rye leaves form oligomeric complexes. Plant Physiol. 119, 1361–1370.

Zhang, T., Yao, Y.-F., 2015. Endophytic fungal communities associated with vascular plants in the high arctic zone are highly diverse and host-plant specific. PLOS One 10, e0130051.
Zhang, Y., Chen, W., Sang, X., Wang, T., Gong, H., Zhao, Y., Zhao, P., Wang, H., 2021. Genome-wide identification of the thaumatin-like protein family genes in gossypium barbadense and analysis of their responses to verticillium dahliae infection. Plants (Basel) 10.
Zhou, S., Cong, L., Liu, J., Zhang, Z., 2022. Consistency between deposition of particulate matter and its removal by rainfall from leaf surfaces in plant canopies. Ecotoxicol. Environ. Saf. 240, 113679.